UNIVERSIDADE DE LISBOA
FACULDADE DE CIÊNCIAS
DEPARTAMENTO DE BIOLOGIA VEGETAL

New reporters for antibiotic discovery

Andreia Monteiro Duarte

Mestrado em Microbiologia Aplicada

Dissertação orientada por:
Prof. Doutora Mariana Pinho
Prof. Doutora Raquel Sá-Leão

2018

Acknowledgments

Firstly, I would like to thank FCUL and ITQB for allowing me to develop my research and to achieve my master's degree. To my supervisor Dr Mariana Pinho, thank you for the amazing opportunity of conducting the thesis at her laboratory, for always demanding high quality work while giving me the chance to perform extra experiments, for sharing her vision, knowledge, curiosity and enthusiasm about the work. As well as for taking her time to teach me, making relevant suggestions and corrections during the past year. To my internal supervisor Dr Raquel Sá-Leão, thank you for her assistance, availability, concern and interest in my thesis. I would also like to thank Dr Sérgio Filipe for sharing his perspectives and for all his questions during lab meetings. To the members of the Bacterial Cell Biology and Bacterial Cell Surfaces and Pathogenesis laboratories, every single one of you taught me something very useful for my future in and outside of the scientific world. Thank you very much for the welcoming environment, it greatly influenced my work. I am very grateful for the guidance of Dr Mário Ferreira, a very concerned co-supervisor who apparently doesn't like to be called Dr or Mr. Thank you for all the encouragement, for patiently teaching and showing me the way around the lab, for always reminding me that there are no stupid questions and for the support, whenever needed. I could not have asked for a better co-supervisor. I would also like to express my gratitude to Dr Nathalie Reichmann, who invested some of her time to discuss about my work, which allowed me to overcome some obstacles during experiments. Thank you for kindly being so interested, for contributing tremendously to the great work environment and for the opportunity to, briefly, work with the Elyra. To Pedro Fernandes, Raquel Pereira, Bruno Saraiva and João Monteiro, thank you for their assistance and availability either with microscopy or bioinformatic issues and for also having always been willing to help. To Andreia Tavares and Ambre Jousselin, thank you for all their support and, of course, for sharing chocolate and other healthy delicacies. Again, thank you to all the members of BCB and BCSP who I had the pleasure to meet.

To my best friend Tiago, we have known each other for some time, so for now I will thank you for keeping me updated, along this year, on which is the next film to watch together and for making sure I would not miss it. To Marianinha, a good friend from Margem Sul, thank you for sharing the same worried mindset, for always sending me photos of new places we have to go and try different types of food and, obviously, for calling to check on how I was doing. To the girls from Portalegre, my friends and colleagues, Margarida and Andreia, and the bookworm Sofia, thank you for all the laughs and for trying to keep in touch. I trully appreciate your friendship and all the time we spend chatting and laughing about the silly things. I will always try to make some time for coffee or drinks with you. To Ana Sofia and Ricardo, thank you for our Saturday afternoons, for discussing your daily struggles, listening to mine and for allowing me to be Sakura's "godmother". A very special thank you to Mr Carlos Pantana, a hockey enthusiast and an unexpected a friend, who introduced me to an extraordinary group of people who, at the end of the day, help one another in everyway they can.

Finally, thank you to all my family, especially to my very loving parents, for their unconditional support and trust. Trying to understand the schedule of their daughter's work was somehow a challenge, as they have never stopped worrying about everything. Thank you for being the best parents ever, for having taught me the meaning of hard-work, perseverance and personal responsibility, the value of speaking truthfully and always being polite to others. Thank you for always being there for me and for showing how rewarding it can be to follow and achieve your goals. Thank you for everything.

New reporters for antibiotic discovery

Andreia Monteiro Duarte

MASTER THESIS

2018

This thesis was fully performed at the Bacterial Cell Biology laboratory at ITQB NOVA under the direct supervision of Prof Dr Mariana Pinho and Dr Mário Ferreira.

Prof Dr Raquel Sá-Leão was the internal designated supervisor in the scope of the Master in Applied Microbiology of Faculdade de Ciências da Universidade de Lisboa.

Abstract

The global threat of multidrug resistant *Staphylococcus aureus* to healthy individuals poses a pressing need to develop new tools and explore alternative targets for the discovery of new antibiotics derived from natural compounds against this human pathogen.

In this work we aimed to construct new tools for antibiotic discovery by constructing reporter strains, in the background of methicillin-resistant *S. aureus* strain JE2, which sense inhibition/damage of essential metabolic pathway/structures in the bacterial cell. Bacteria respond to various environmental stresses by triggering the expression of specific genes. We have focused on the response to loss of membrane potential and inhibition of fatty acid biosynthesis and constructed reporter *S. aureus* strains that become fluorescent upon detection of compounds causing these phenotypes. This was achieved by placing the gene encoding the fluorescent protein mNeonGreen under the control of the *lrg* and *fap* promoters that respond to loss of membrane potential and inhibition of fatty acid biosynthesis, respectively. The *lrg* operon takes part in the response of LytSR, a two-component regulatory system that senses the decrease of membrane electric potential due to the ever-changing environmental conditions. This response is based on the activity of Lrg proteins, which attempt to prevent cell membrane permeabilization and therefore ensure survival of stressed bacterial cells. The *fap* regulon is monitored by FapR, a repressor which controls the status of fatty acid biosynthesis and phospholipid metabolism. When a compound interferes with this pathway, intracellular levels of malonyl-CoA increase and FapR repression is inhibited, allowing *fap* genes expression. We concluded that induction of mNeonGreen expression driven by the *lrg* promoter upon loss of membrane potential was too weak for these reporter strains to be used in high-throughput screenings. However, induction of *fap* led to a two-fold increase of cells fluorescence, indicating that this is a promising tool for the discovery of antimicrobial compounds that act through inhibition of fatty acid biosynthesis.

Keywords: *Staphylococcus aureus*; multidrug resistance; cell membrane homeostasis; membrane potential; fatty acid biosynthesis

Resumo

Staphylococcus aureus é uma bactéria patogénica nosocomial, versátil e com grande capacidade de adaptação a diversos ambientes. A penicilina constituiu a primeira linha de tratamento eficaz contra graves infeções causadas por esta bactéria. No entanto, a evolução da mesma levou ao aparecimento e posterior disseminação de estirpes produtoras de penicilinases. De forma a contornar este problema inicial de resistência antimicrobiana, foram desenvolvidos compostos sintéticos derivados da penicilina, nomeadamente, meticilina e oxacilina. Estes compostos passaram a ser utilizados como terapia antimicrobiana contra infeções de estirpes resistentes à penicilina. O uso clínico destes antibióticos conduziu à emergência de estirpes resistentes à meticilina *(methicillin-resistant Staphylococcus aureus* - MRSA) e subsequente evolução da sua resistência a todos os antibióticos disponíveis. Posteriormente, ocorreu a disseminação da multirresistência de algumas destas estirpes até à situação atual, o que levou a um aumento, à escala mundial, da mortalidade associada a infeções causadas por *S. aureus*, mesmo em indivíduos considerados saudáveis (sem outras patologias associadas). Dado que esta bactéria patogénica surge em formas resistentes a vários antibióticos, aos quais era previamente suscetível, o número de opções de tratamento ao qual se pode recorrer é reduzido, sendo na maioria dos casos utilizada vancomicina, ou alternativamente daptomicina e linezolida. Contudo, já existem casos e estudos de estirpes de *S. aureus* resistentes a estes compostos. Embora em Portugal a prevalência de MRSA esteja aparentemente a diminuir, estas estirpes continuam a ser um problema bastante grave, correspondendo a cerca de 50% das estirpes isoladas, o que constitui um dos números mais elevados a nível europeu. Deste modo, a investigação de novas estratégias que permitam o tratamento eficaz destas infeções é de elevada importância. Para o desenvolvimento de novos tratamentos antimicrobianos é necessário compreender não só os mecanismos de ação dos antibióticos, como também os que estão subjacentes à resistência aos mesmos e que foram adquiridos por *S. aureus*.

O problema mundial da (multi)resistência a antibióticos em conjunto com as dificuldades recorrentes em descobrir novos compostos eficazes no combate a infeções microbianas, requerem a urgente inovação no desenvolvimento de técnicas que auxiliem no processo de identificação de novos alvos. Limitações na diversidade de químicos eficazes e identificação de alvos, juntamente com reduzidas concentrações disponíveis de produtos naturais, levaram à estagnação do processo de descoberta de antibióticos. Como tal, as técnicas base envolvidas na descoberta de compostos antimicrobianos são atualmente combinadas, de forma a contornar as suas restrições individuais e possibilitar resultados mais robustos. Os ensaios de *screening* direcionados a alvos específicos são um exemplo claro desta inovação, analisando e comparando a resposta de estirpes geneticamente modificadas com a da estirpe parental. Podendo utilizar sistemas de fluorescência ou de bioluminescência e requerendo quantidades reduzidas de compostos de interesse/a testar durante os estudos/ensaios, este tipo de estirpes modificadas constituem ferramentas úteis para a descoberta de antibióticos, nomeadamente compostos derivados de produtos naturais. Considerando os alvos clássicos de antimicrobianos, estes tipos de *screening* realizados em células bacterianas possibilitam a descoberta de novos compostos que atuem em enzimas e/ou estruturas envolvidas na síntese da parede celular, metabolismo do ácido fólico, ribossomas, polimerases do RNA, entre outros alvos mais comuns. Todavia, ao aplicar estes *screenings* a alvos menos estudados e que estão envolvidos em processos igualmente essenciais como, por exemplo, a divisão celular, homeostasia da membrana celular ou biossíntese de ácidos gordos, poderão ser descobertos novos compostos, ou formas mais eficazes de utilizar os já conhecidos, para o tratamento de infeções por MRSA.

Devido à constante interação com o ambiente externo e fatores de stress associados, as bactérias utilizam diversos mecanismos para manter a integridade celular, nomeadamente membranar, assegurando, assim, a sua sobrevivência. A membrana citoplasmática está, por isso, envolvida em

inúmeros processos desde o transporte de moléculas, respiração, comunicação celular, produção de energia, até à manutenção da força protomotriz. A alteração do potencial de membrana, uma das componentes da força protomotriz, é integrada como estímulo ambiental pela cinase de histidina LytS do sistema regulatório LytSR, que posteriormente desencadeia (via LytR) a reposta celular adequada. Outra forma possível de ativar e induzir uma resposta do sistema LytSR tem por base a fosforilação do regulador de resposta LytR como resultado da acumulação metabólica de acetato em células que se encontram na presença de concentrações elevadas de glucose. A resposta celular mediada por LytR consiste na ativação dos genes do operão *lrgAB*. Este operão está envolvido na regulação do programa de morte celular programada e tolerância a antibióticos, como a penicilina, funcionando de modo oposto ao operão *cidABC* dado que os produtos destes genes são homólogos aos sistemas de bacteriófagos de antiholinas e holinas, respetivamente. Quando LytS deteta a dissipação do potencial de membrana, fosforila o ativador LytR que irá, consequentemente, induzir a expressão dos genes *lrg*. LrgA funciona como uma antiholina, contrariando o efeito de permeabilização membranar da holina CidA, impedindo, assim, a morte celular e subsequente lise.

Outro parâmetro que contribui para a sobrevivência e homeostasia da membrana celular é a composição lipídica da mesma. As bactérias produzem ácidos gordos e fosfolípidos através de um sistema diferente do dos seres humanos e outros organismos eucariotas, sendo o metabolismo destes lípidos controlado pelo regulão *fap* desse mesmo sistema. No centro desta regulação encontra-se o repressor FapR, capaz de regular a sua própria expressão através do controlo do gene *fapR* que o codifica. Deste modo, a indução do regulão, por compostos que inibam as enzimas desta via de biossíntese lipídica, é conseguida após inibição da atividade do FapR. Por sua vez, repressão mediada pelo FapR é inibida aquando do aumento dos níveis intracelulares de malonil-CoA, um intermediário da biossíntese de ácidos gordos e fosfolípidos, cuja concentração pode ser aumentada ao bloquear/inibir um dos passos enzimáticos da via. Devido à importância desta via para a estabilidade/homeostasia da estrutura membranar, as várias enzimas da biossíntese de ácidos gordos e fosfolípidos podem teoricamente ser consideradas como alvos eficazes de antibióticos.

O presente trabalho tem por objetivo a construção de novas ferramentas para a descoberta de compostos antimicrobianos através da modificação genética da estirpe MRSA JE2, de forma a construir novas estirpes repórter fluorescentes. Deste modo, as estirpes repórter construídas serão capazes de detetar a inibição ou dano de vias metabólicas ou estruturas essenciais para a célula bacteriana. Como a resposta bacteriana a vários estímulos ambientais tem por base a indução da expressão de genes específicos, neste trabalho foram escolhidos os sistemas ou vias que respondem à diminuição ou perda de potencial de membrana e à inibição da biossíntese de ácidos gordos para construção das estirpes repórteres. Desta forma as bactérias repórter construídas ficam fluorescentes após deteção de compostos que causam os fenótipos anteriores, e a sua resposta é quantificável com base na fluorescência apresentada. Para construção dos repórteres, o gene que codifica a proteína mNeonGreen foi colocado sob o controlo dos promotores do operão *lrg* e do regulão *fap*, que respondem à redução do potencial de membrana e inibição da síntese de ácidos gordos, respetivamente.

Nesta dissertação, concluímos que a indução da expressão de mNeonGreen sob o controlo do promotor de *lrg* após diminuição do potencial de membrana era demasiado reduzida para este repórter ser considerado adequado num *screening* de bibliotecas de compostos naturais. Todavia, os resultados da indução do repórter *fap* apontam para uma duplicação dos níveis de fluorescência das células, o que indica que esta estirpe é uma ferramenta promissora para a descoberta de compostos antimicrobianos que atuam através da inibição da via de biossíntese dos ácidos gordos.

Palavras-chave: *Staphylococcus aureus*; multirresistência a antibióticos; potencial de membrana; biossíntese de ácidos gordos; homeostasia da membrana celular.

Table of Contents

Acknowledgments III
Abstract VII
Resumo IX
Table of Contents XI
List of Tables XII
List of Figures XIII
List of Symbols and Abbreviations XV
1. Introduction 1
1.1. *Staphylococcus aureus*, a case of evolution of antibiotic resistance 1
1.2. Targets and tools for antibiotic discovery 2
1.3. Membrane potential is essential for cell survival 3
1.4. Essentiality of fatty acid biosynthesis 6
1.5. Aims 7
2. Materials and Methods 8
2.1. Bacterial strains and growth conditions 8
2.2. Molecular Cloning 9
2.2.1. DNA manipulation 9
2.2.2. *E. coli* transformation 9
2.2.3. *S. aureus* transformation and transduction 9
2.3. Construction of reporter *S. aureus* strains 10
2.4. Determination of minimum inhibitory concentrations 12
2.5. Growth analysis of *S. aureus* strains 12
2.6. *fabZ* antisense RNA induction 12
2.7. Fluorescence microscopy 12
2.8. Fluorimeter analysis 13
2.9. Statistical analysis 13
3. Results 14
3.1. Construction of mNeonGreen reporter strains 14
3.2. Induction of *lrg* reporter 16
3.3. Alternative *lrg* reporter 20
3.4. Induction of *fap* reporter 22
3.5. Initial optimization for subsequent high-throughput screening 25
3.6. Daptomycin fluorescence 26
4. Discussion and Conclusions 28
5. References 31
6. Supplementary Information 37

List of Tables

Table 2.1. Bacterial strains and plasmids.

Table 2.2. Primers used for construction of *S. aureus* reporter strains.

Table 3.1. MICs of reporter strains to compounds that affect membrane potential or fatty acid biosynthesis.

Supplementary Table 1. MICs of reporter strains to compounds that affect membrane potential or fatty acid biosynthesis in TSB.

List of Figures

Figure 1.1. The two pathways for activation of LytR.

Figure 1.2. Balance between holin-like CidA and antiholin-like LrgA.

Figure 1.3. Bacterial type II fatty acid biosynthesis pathway.

Figure 3.1. Schematic representation of the chromosomal organization of strains expressing different promoter fusions.

Figure 3.2. Growth curves of *lrg* reporter strains.

Figure 3.3. Growth curves of P_{fap} reporter strain.

Figure 3.4. Microscopy images of JE2_Plrg_mNeonGreen exposed to daptomycin.

Figure 3.5. Microscopy images of JE2_Plrg_mNeonGreen exposed to CCCP.

Figure 3.6. P_{lrg} promoter activity in the absence or presence of daptomycin and CCCP.

Figure 3.7. Microscopy images and quantification of P_{lrg} promoter activity of JE2_Plrg_mNeonGreen exposed to glucose, acetate and bicarbonate.

Figure 3.8. Microscopy images of JE2_lrgB_mNeonGreen exposed to daptomycin.

Figure 3.9. Microscopy images of JE2_lrgB_mNeonGreen exposed to CCCP.

Figure 3.10. Promoter activity of *lrgB* fusion to *mmeongreen* in the absence or presence of daptomycin and CCCP through quantification of mNeonGreen fluorescence.

Figure 3.11. Microscopy images of JE2_Pfap_mNeonGreen exposed to triclosan.

Figure 3.12. P_{fap} promoter activity in the absence or presence of triclosan through quantification of mNeonGreen fluorescence.

Figure 3.13. Microscopy images of *fabZ* RNA antisense induction of fap reporter strain.

Figure 3.14. P_{fap} promoter activity upon induction of *fabZ* antisense RNA and fluorescence from mNeonGreen expression was quantified.

Figure 3.15. Quantification of mNeonGreen fluorescence levels of JE2_Pfap_mNeonGreen in the absence or presence of triclosan using a fluorimeter microplate system.

Figure 3.16. Microscopy images of JE2 exposed to CCCP and daptomycin.

Figure 3.17. Microscopy images of JE2 exposed to daptomycin.

Figure 4.1. Scheme of RNA polymerase binding sites for each *lrg* reporter strategy.

Supplementary Figure 1. Growth curves of P_{fap} reporter strain in TSB.

Supplementary Figure 2. P_{lrg} promoter activity in the absence or presence of CCCP during short periods of incubation.

Supplementary Figure 3. P_{lrg} promoter activity in the absence or presence of supra-MIC conditions of inducer during 45 min.

Supplementary Figure 4. Growth curves of JE2 in both MHB and Ca-MHB.

List of Symbols and Abbreviations

ΔΨ	membrane electric potential	**DNA**	deoxyribonucleic acid
ΔpH	transmembrane proton gradient	**EDTA**	ethylenediaminetetraacetic acid
::	insertion	**FASII**	type II fatty acid biosynthesis pathway
Δ	deletion	**GFP**	green fluorescent protein
ϕ	bacteriophage	**HA-MRSA**	hospital-acquired methicillin-resistant *Staphylococcus aureus*
°C	Celsius degree	**HTS**	high-throughput screening
%	percentage	**LA**	lysogeny agar
bp	base pair	**LB**	lysogeny broth
g	gravitational force	**MIC**	minimum inhibitory concentration
h	hour	**MHB**	Mueller Hinton broth
min	min	**MOA**	mechanism of action
mg	milligram	**mRNA**	messenger ribonucleic acid
mL	millilitre	**MRSA**	methicillin-resistant *Staphylococcus aureus*
mM	millimolar	**NAD^+**	oxidized form of nicotinamide adenine dinucleotide
ms	millisecond	**OD**	optical density
M	molar	**PBP**	penicillin-binding protein
µg	microgram	**PBS**	phosphate-buffered saline
µL	microlitre	**PCR**	polymerase chain reaction
µm	micrometre	**PG**	phosphatidylglycerol
nm	nanometre	**PGN**	peptidoglycan
rpm	revolutions per minute	**PMF**	proton motive force
ATP	adenosine triphosphate	**RBS**	ribosome binding site
Ca-Dap	calcium-Daptomycin complexes	**RNA**	ribonucleic acid
Ca-MHB	Mueller Hinton broth	**TCRS**	two-component regulatory system
CA-MRSA	community-acquired methicillin-resistant *Staphylococcus aureus*	**TSA**	tryptic soy agar
CCCP	carbonyl cyanide *m*-chlorophenylhydrazone	**TSB**	tryptic soy broth
CL	cardiolipin	**WT**	wild-type
DAPI	4’,6-diamidino-2-phenulindole	**X-Gal**	5-bromo-4-chloro-3-indolyl β-D-galactopyranoside

1. Introduction

1.1. *Staphylococcus aureus*, a case of evolution of antibiotic resistance

Originally described and classified by Rosenbach[1], S*taphylococcus aureus* is a Gram-positive cocci-shaped bacterium with low GC genomic content. As a commensal bacterium present in the normal microbiota of humans, *S. aureus* commonly colonizes mucosal surfaces and the skin[2] of nearly 30% of the human population[3,4]. To go from colonization to infection, this bacterium only requires a window of opportunity, *i.e.*, a breach in the host's defences to act as a pathogen[3]. *S. aureus* is an extremely versatile pathogen, responsible for numerous cases of skin infections, pneumonia, endocarditis, pyaemia, bacteraemia, septicaemia, toxic shock syndrome, and is one of the major causes of nosocomial infections[2,5,6]. Staphylococci transmission between individuals mainly occurs through skin-to-skin contact or contaminated objects[6,7].

Prior to the antibiotic era, *S. aureus* versatility greatly concerned clinicians due to 75% or higher bacteraemia mortality rates[8]. In 1929, Alexander Fleming accidently discovered penicillin while observing the inhibition halo in staphylococci plates contaminated with *Penicillium* mould. The antibacterial activity of penicillin is known to target the synthesis of the cell wall of bacteria. Specifically the β-lactam ring irreversibly inactivates penicillin-binding proteins (PBPs), preventing their transpeptidase catalytic activity, *i.e.*, inhibiting the crosslinking of peptidoglycan (PGN), weakening the cell wall and leading to cell lysis[9,10].

From 1939, penicillin started being used to treat staphylococcal and other Gram-positive infections[11]. Reflecting its efficacy, penicillin was afterwards extensively used worldwide and thus the first hospital isolated *S. aureus* strains exhibiting resistance to penicillin were reported shortly after, in 1946[12]. These first resistant strains contained a plasmid which encoded for a β-lactamase, *i.e.*, a penicillase capable of inactivating the antimicrobial activity of penicillin by hydrolysing its β-lactam ring[13]. Consequently, penicillin-resistant strains spread throughout the community to a point where more than 80% of hospital and community *S. aureus* isolates were resistant to the β-lactam[14]. Since penicillin treatment was no longer effective against staphylococcal infections, synthetic β-lactamase-resistant penicillins were developed, such as methicillin and oxacillin[15]. However, a few years after the introduction of these new β-lactams, the first methicillin-resistant *Staphylococcus aureus* (MRSA) strain was isolated from a hospital patient in Colindale, United Kingdom. This hospital-acquired MRSA (HA-MRSA) strain was named COL and is still one of the most studied MRSA strains[16,17]. Even though its resistance mechanism was not based on antibiotic degradation, the β-lactams methicillin, cephalosporins and carbapenems were ineffective against this MRSA strain[18]. Clones of *S. aureus* COL spread around the globe, which greatly contributed to the increasing number of nosocomial infections by resistant strains[19]. The situation aggravated into the current existence of *S. aureus* strains which are virtually resistant to all known antibiotics[20], more commonly known as multidrug resistant *Staphylococcus aureus*. Another consequence was the non-exclusivity of MRSA to hospital environments. The first infection case of a healthy individual with a community-acquired MRSA (CA-MRSA) strain was reported in the 1980s[21]. Although CA-MRSA strains are usually less resistant to β-lactams[22,23], they tend to be more virulent and infect healthy individuals[24,25]. Community MRSA clones are typically non–multidrug resistant[22]. However, clones of these strains have also spread into clinical settings, successfully causing nosocomial infections and healthcare-associated bacteremias. One of these strains is USA300 (or JE2)[26,27], which emerged as an epidemic clone in the USA[28], but has since been reported in Europe, South America, Asia and Australia[29–31].

After the spread of MRSA strains, the only effective antibiotic against these strains was vancomycin. As β-lactams, vancomycin also targets the synthesis of the bacterial cell wall, but via a different mechanism: this glycopeptide prevents both transglycosylation (elongation of PGN chains)

and transpeptidation (PGN cross-linking) enzymatic activities by binding directly to the dipeptide D-Ala4-D-Ala5 of the precursor for cell wall synthesis, lipid II[32]. However, with the increased and prolonged use of vancomycin in hospital facilities (higher selective pressure), intermediate and vancomycin-resistant *S. aureus* strains emerged[33,34]. This resistance was even reported in some isolates of USA300[35], but fortunately these strains have not become prevalent[20]. As MRSA strains have demonstrated resistance to the entire class of penicillin-like antibiotics and to glycopeptides, like vancomycin, and others[36], daptomycin and linezolid are currently used as alternative anti-MRSA therapies[20]. Nevertheless, with its use, even resistance to these antibiotics has been reported and studied[37–39].

The struggle to find new effective antimicrobials is based on the fundamental fact that exposure to antibiotics will eventually lead to tolerance or even resistance by the pathogen[24,40,41]. This never-ending cycle has considerable economic and clinical implications. In 2005, the CDC reported 18 650 estimated deaths due to *S. aureus* infections in the USA[28], while tuberculosis was the official cause of less than 700 American deaths[42]. In Europe, there is a great variability of CA-MRSA clones, being USA300 or related clones the most predominant[43]. Although the prevalence of MRSA in Portugal has been diminishing, these strains still constitute a serious issue: 50% of detected *S. aureus* strains are resistant to methicillin[44]. For that reason, treatment of patients with *S. aureus* infections resistant to almost all known antibiotics urgently needs to be attended. A better understanding of recent resistance mechanisms of *S. aureus*, especially in MRSA strains, and search for new antibiotic therapies may contribute to prevent and more effectively treat staphylococci infections.

1.2. Targets and tools for antibiotic discovery

As mentioned above, β-lactams were the first antibiotics to be used as treatment for Gram-positive infections, namely the naturally produced penicillin. However, the Golden Age of antibiotic discovery suffered a decline after the late 70s, quickly shifting to an innovation gap which eventually led to the so-called discovery void [45,46]. Therefore, during the past 40 years antibiotic resistance has been a global issue, whereas the discovery of new antimicrobials remains mostly stagnated since it is much easier to find compounds that kill bacteria non-specifically, such as non-target specific detergents, than finding new antibacterial classes worthy of development[46].

The major bottlenecks in drug discovery are target identification and limited diversity of chemicals[46], with the additional challenge of natural products being present in low concentrations in extracts. Conventionally, discovery of natural products was based in desired phenotypic effects, either by empirical screening using inhibition of growth assays, without knowledge of mechanism of action (MOA), or by *in vitro* biochemical assays of enzymatic inhibition [46,47]. Even though *in vivo* assays were useful for the identification of numerous natural products, assessment of whole-cell activity frequently resulted in the discovery of nonspecific toxic compounds[48].

The development of target-based biochemical and macromolecular strategies allowed specific knowledge of target-antibiotic affinity and activity. However, *in vitro* assays failed to address permeability of *in vivo* barriers and frequency of resistance through efflux upon compound entry in the cells[46,49]. Another limitation is that *in vitro* assays identify compounds with specific MOAs against single targets, which result in the development of resistance at higher frequencies than what is accepted for clinical use[46,47].

Evidently, *in vitro* and *in vivo* techniques complement each other by circumventing individual limitations, which eventually resulted in target-directed phenotypic screenings. These assays are usually based in the analysis of differences between a wild-type (WT) parental strain and a genetically engineered reporter strain. The bioreporter strains may be drug resistant, overexpress a selected target

or deleted of a gene of interest[48]. These reporter strains can be genetically modified to produce an easily quantifiable dose-dependent signal in response to the presence of the inducing chemical or stress factor[50,51]. One approach is to genetically modify bacteria by fusing a promoter sequence (previously known to respond to the target compound) to a reporter system such as *gfp*, *mneongreen*, or *mcherry* for fluorescence or the *luxCDABE* genes for bioluminescence. Such reporter bacteria have been useful tools for antibiotic discovery[52]. Recent studies use bioreporter bacteria either harbouring reporter plasmids[51,53] or having integrated reporters into the genome[54,55]. With a definition of MOA from the onset, reporter gene assays allow further analysis on cell morphology changes and specific phenotypic alterations due to inhibition of precise pathways[48,56]. Whole-cell mechanism-based screenings combined with reporter assays provide a better characterization of MOA and potential applicability to any desired target, while often requiring low amounts of compounds of interest, namely from natural microbial extracts.

The common/classic targets of antibiotics are enzymes involved in bacterial cell wall synthesis, enzymes of folic acid metabolism, topoisomerases, RNA polymerases, ribosomes and other protein synthesis machinery/molecules. As mentioned previously β-lactams and vancomycin inhibit synthesis of PGN. Linezolid binds to peptidyl transferase centre in the 50S ribosome subunit, inhibiting translation of mRNA/protein synthesis. Nonetheless, there are already reports and, in most cases, studies on the resistance mechanisms adopted by *S. aureus* for the majority of natural and synthetic compounds that act on these targets[20]. Still, old targets can continue to be explored. A recent screening study reported teixobactin as a new lipid II inhibitor that therefore inhibits PGN biosynthesis, to which *S. aureus* does not display resistance[57,58].

Besides trying to find new compounds against old targets, we should also consider methods that allow discovery of antibiotics that act on unexplored/less explored targets, such as cell division, persistence mechanisms, teichoic acid biosynthesis, fatty acid synthesis and membrane stability/integrity[20].

In this thesis, we chose to develop reporters for compounds that act through two MOA, closely involved with the bacterial cytoplasmic membrane: loss of membrane potential and inhibition of phospholipid biosynthesis.

1.3. Membrane potential is essential for cell survival

The cytoplasmic membrane of bacteria is directly involved in the transport of nutrients and metabolic "waste" products, respiration, production of ATP and cell-cell communication, as well as in establishing a proton motive force (PMF), a key parameter for the energetic pathway of cell membranes[59]. Required for several cellular processes, the PMF can be defined as an electrochemical gradient of protons resulting from proton extrusion by the electron transport chain. The PMF has two components: the electric potential ($\Delta\Psi$, membrane potential) and the transmembrane proton gradient (ΔpH)[60]. Furthermore, membrane potential has an important role in modulating the distribution of several proteins during cell division[61].

Perturbation of the cell membrane electrical potential is sensed by the *S. aureus* LytSR two-component regulatory system (TCRS)[62], which is also involved in adaptation of these bacteria to cationic antimicrobial peptides that are released by the host innate immune system after colonization by *S. aureus*[63]. Upon recognition of $\Delta\Psi$ disruption, the membrane-bound histidine kinase LytS autophosphorylates a conserved histidine residue at position 390 (His390) (Figure 1.1.). Acting as phosphodonor, phosphorylated LytS transfers the phosphate to a conserved aspartate residue at position 53 (Asp53) of the response domain of the regulator LytR (primary pathway). LytS also displays phosphatase activity that may contribute to regulate LytR dephosphorylation[64,65]. Additionally, *in vitro* and *in vivo* studies report phosphorylation of the activator LytR through acetyl phosphate as a result of

accumulation of acetate during metabolism in the presence of excess glucose, a LytS-independent activation pathway (secondary pathway)[64,65].

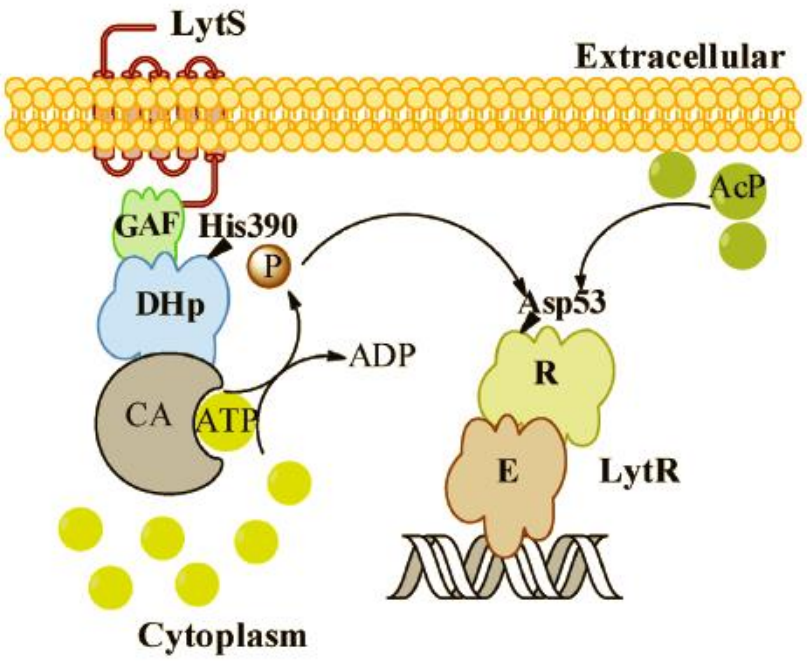

Figure 1.1. The two pathways for activation of LytR. The primary pathway consists on signal transduction from the sensor kinase LytS to the effector LytR, *i.e.*, phosphorylation of LytR by LytS after sensing changes on membrane potential, whereas the secondary pathway is based on LytR phosphorylation via acetyl phosphate (AcP) in response to excess of glucose metabolism. The activated LytR will then bind to promoters regulated by LytSR two-component regulatory system. Protein domains: GAF – cyclic Guanosine monophosphate specific phosphor-diesterases, Adenylyl cyclases and the Fhl; DHp – Dimerization and Histidine phosphotransfer; CA – Catalytic and ATP-binding; R – Receiver, E – Effector [64].

One of the operons regulated by the LytSR TCRS is the dicistronic *lrgAB* (*lrg*) operon, which is immediately downstream of *lytR* in the chromosome of *S. aureus*[64,66]. Through the effector domain, the phosphorylated LytR will then bind to DNA adjacently to the promoter (P_{lrg}) of the *lrg* operon and allowing its activation[64,66].

The *lrg* operon takes part in murein hydrolase activity, penicillin sensitivity[67], and, along with the *cid* operon, regulates the balance between autolysis rate during programmed cell death and biofilm formation[68,69]. While *cid* gene products enhance murein hydrolase activity and antibiotic tolerance, the *lrg* gene products inhibit these same processes in a similar way to bacteriophage-encoded holins and antiholins, respectively[67,70]. Holins oligomerize in the bacterial cytoplasmic membrane causing cell death and, due to their effects on murein hydrolase activity, cell lysis. Antiholins inhibit holin oligomerization and, therefore, prevent bacterial death and lysis.

Therefore, it has been proposed that LytS detects and responds to $\Delta\Psi$ dissipation through phosphorylation of LytR, proceeded by LytR induction of the antiholin-like protein LrgA and its cellular attempt to prevent total membrane permeabilization caused by oligomerization of holin-like CidA proteins (Figure 1.2.)[68,71].

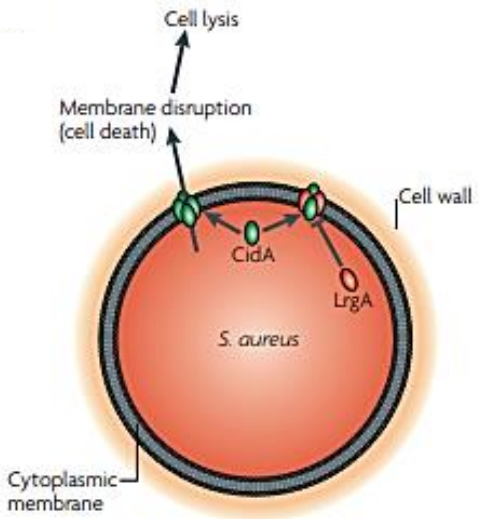

Figure 1.2. Balance between holin-like CidA and antiholin-like LrgA. The *Staphylococcus aureus* proteins CidA and LrgA are considered to function as a holin and antiholin, respectively. CidA controls the timing of cell death and lysis through oligomerization at the cytoplasmic membrane, whereas LrgA is a homologous protein which has an inhibitory effect on CidA holin activity [68].

Under specific stress conditions, P_{lrg}-controlled genes respond to compounds that target membrane potential like the lipopeptide daptomycin or the protonophore carbonyl cyanide *m*-chlorophenylhydrazone (CCCP)[72–74]. CCCP is an uncoupling agent capable of diffusion across the cytoplasmic membrane in either of its forms. In response to a pH gradient, the protonated form of CCCP easily diffuses into the cell where it releases a proton, whereas the non-protonated form is protonated at the external surface of the membrane prior to diffusion across it[72]. It has been reported that CCCP-induced P_{lrg} activity and subsequent *lrgAB* expression are dependent on the LytS signal transduction[65].

The cyclic lipopeptide daptomycin is used to treat infections with Gram-positive bacteria, namely MRSA strains[75–77]. This anionic compound requires calcium ions for its antimicrobial activity[78]. However, the MOA of daptomycin is not yet fully understood. This antibiotic may have a dual action, targeting both the cytoplasmic membrane and the cell wall[73,79].

Daptomycin is able to destabilize the membrane by formation of calcium-daptomycin complexes (Ca-Dap) and interaction with phosphatidylglycerol (PG, a negatively charged phospholipid and the most abundant in the membrane of *Staphylococcus*), resulting in decrease or complete dissipation of membrane potential (so called disruption) and cell death[78]. This membrane-targeting MOA is supported by resistance studies in Gram-positive bacteria, which show a correlation between increased daptomycin resistance and more positively-charged cell membranes[79–81]. These studies show that daptomycin-resistant strains frequently exhibit single mutations in the multipeptide resistance factor gene (*mprF*), which is responsible for the synthesis and translocation of the positively charged phospholipid, lysyl-phosphatidylglycerol, to the outer surface of the cell membrane, increasing its charge and therefore repelling Ca-Dap[37,82]. Firstly discovered in enterococci, genetic cues for an alternative strategy to change membrane lipid composition were also found in *S. aureus*. Activity-enhancing mutations in cardiolipin synthase may alter the ratio of PG:CL in the membrane, allowing the subsequent protective effect of cardiolipin (CL, another negatively charged phospholipid present in *Staphylococcus* membrane) against Ca-Dap complexes[81,83]. Another membrane-changing mechanism associated with resistance to daptomycin is the alteration from a fluid to an excessively rigid state of the membrane as a result of increased production of the carotenoid staphyloxanthin[37,84].

Daptomycin can also lead to aberrant cellular morphologies, with abnormal division septa and bulging membranes without lysis[84–87]. Further studies on the subject led to the proposal of a new resistance mechanism of *S. aureus* through membrane phospholipid shedding which sequestered and inactivated daptomycin[38]. Besides the *lrg* operon, transcriptional-profiling analysis showed that daptomycin also induces cell wall-related genes[73,88], raising the possibility that daptomycin directly or indirectly inhibits PGN synthesis.

1.4. Essentiality of fatty acid biosynthesis

The bacterial synthesis of fatty acids has been exploited for development of new compounds to treat staphylococci infections. Contrary to humans, bacteria produce their own fatty acids through the type II fatty acid synthesis pathway (FASII), presenting multiple and common targets for antibiotic discovery. Moreover, the most effective known antimicrobials against FASII are natural products [89,90]. In *S. aureus* the cyclic elongation step of fatty acid biosynthesis is performed by four enzymes encoded by the *fap* regulon: FabG, FabZ, FabI and FabF (Figure 1.3.)[89,90].

In Gram-positive bacteria, the *fap* regulon is constituted by six operons and the *fab* genes are responsible for converting acetyl-CoA or malonyl-CoA into the long-chain fatty acids (Figure 1.3.). Largely conserved in bacteria, including *S. aureus*, the global regulator of FASII is the fatty acid and phospholipid regulator (FapR). Hence, induction of *the fap* regulon is performed by inactivating the transcriptional repressor FapR and, consequently, allowing an increased expression of genes belonging to the *fap* regulon. FapR, which also regulates the expression of its own encoding gene, *fapR*, binds to a consensus 17 bp inverted repeat DNA sequence that is highly conserved in several Gram-positive bacteria[91,92].

In vitro transcription assays of several promoters of the *fap* regulon demonstrated that increased levels of malonyl-CoA (Figure 1.3.), an intermediate in fatty acid biosynthesis, lead to a decreased FapR-mediated repression of the *fap* regulon[91,93]. This vital effector and intermediate of fatty acid synthesis offers a mechanism to monitor/assess phospholipid homeostasis mediated by FapR and, if necessary, subsequently adjust the *fap* regulon expression[92].

Due to the essentiality of this pathway in bacteria, FASII inhibitors have been developed. One of these antimicrobial compounds is triclosan (Figure 1.3.), a widely used biocide and disinfectant agent. At low concentrations triclosan targets FabI and, by forming stable FabI-NAD^+-triclosan ternary complexes, prevents the elongation of the fatty acid chain in the last reaction step of each elongation cycle[94,95]. Inhibition of this step leads to accumulation of malonyl-CoA and, consequently, to increased expression of genes belonging to the fap regulon.

Emergence of triclosan resistant strains, with chromosomal mutations or that harbour a second *fabI*, leading to an increase of the target amount[96], and the ability of *S. aureus* to use lipoproteins of hosts as exogenous fatty acids[97], are relevant to further consider scientific and financial investments in the development of new drugs[98,99]. Nevertheless, triclosan-derived antimicrobials for therapy of staphylococci infections are being developed[100,101], but there is a significant risk that resistance phenotypes emerge due to missense mutations in *fabI*, as these inhibitors have a single target[46,102].

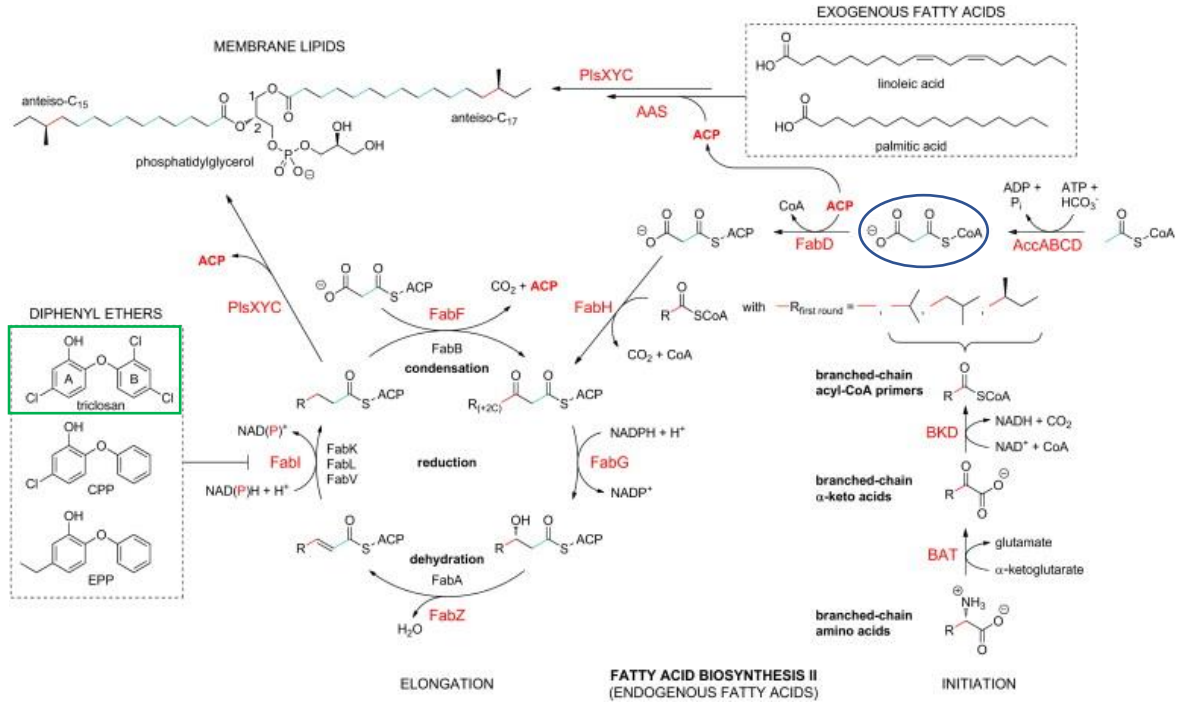

Figure 1.3. Bacterial type II fatty acid biosynthesis pathway. The *Staphylococcus aureus* enzymes are in red and isoforms are in black. Fatty acid biosynthesis starts with acetyl-CoA, which is converted in malonyl-CoA (blue elipse) by acetyl-CoA carboxylase (Acc), and subsequently converted in malonyl-ACP by malonyl-CoA:ACP transacylase (FabD). The β-ketoacyl-ACP synthase (FabH) performs the first condensation reaction. During the first elongation cycle, the β-ketoacyl-ACP is converted to a saturated acyl-ACP by the actions of the NADPH-dependent reductase FabG, the dehydrase FabZ, and the mostly NADH-dependent enzyme FabI. The saturated acyl-ACP is the substrate for additional rounds of elongation in which FabF catalyzes the condensation reaction. The long-chain acyl-ACP products are subsequently partially transformed into membrane lipids (a typical S. aureus phosphatidylglycerol is shown at the top). Contrary to most bacteria, *S. aureus* FabH prefers branched-chain acyl-CoAs which yield branched-chain fatty acids. Triclosan (green rectangle) is one of the inhibitors of the NADPH-dependent FabI from *S. aureus*. BAT – branched-chain aminotransferase; BKD – branched-chain α-ketoacid dehydrogenase; PlsXYC – acyltransferase system; AAS – acyl-ACP synthetase; CPP – 5-chloro-2-phenoxyphenol; EPP – 5-ethyl-2-phenoxyphenol[95].

1.5. Aims

Considering the importance to discover novel antimicrobial compounds, in this work we chose to construct new membrane-related bioreporters and test them by following promoter activity through fluorescence detection, assessing whether these reporters would constitute a good tool for future high-throughput screenings (HTS).

2. Materials and Methods

2.1. Bacterial strains and growth conditions

The bacterial strains and plasmids used during this study are listed in Table 2.1.

Table 2.1. Bacterial strains and plasmids.

Strain/Plasmid	Relevant Characteristics[a]	Source/Reference
Strain		
Escherichia coli		
DC10B	Cloning strain, Δdcm in the DH10B background; Dam methylation only	[103]
DH5α pJ201 mNeonGreen #1	recA endA1 gyrA96 thi-1 hsdR17 supE44 relA1 ϕ80 ΔlacZΔM15 with pJ201 mNeonGreen #1	Gibco-BRL
Staphylococcus aureus		
RN4220	MSSA strain, restriction deficient derivative of NCTC8325-4	[104]
RN4220_Plrg_mNeonGreen	RN4220 with pMAD_Plrg_mNeonGreen	This study
RN4220_lrg_mNeonGreen	RN4220 with pMAD_lrgB_rbs_mNeonGreen	This study
RN4220_Pfap_mNeonGreen	RN4220 with pMAD_Pfap_mNeonGreen	This study
JE2	CA-MRSA USA300 strain	[105]
JE2_Plrg_mNeonGreen	JE2::P_{lrg}-mNeonGreen	This study
JE2_lrgB_mNeonGreen	JE2::*lrgB*-mNeonGreen	This study
JE2_Pfap_mNeonGreen	JE2::P_{fap}-mNeonGreen	This study
JE2 AS-*fabZ*	JE2 with pEPSA::AS-020, Cm^R	This study
JE2_Pfap_mNeonGreen AS-*fabZ*	JE2_Pfap_mNeonGreen with pEPSA::AS-020, Cm^R	This study
Plasmid		
pMAD	Thermosensitive plasmid used for allelic replacement in Gram-positive bacteria, *lacZ*, Amp^R Ery^R	[106]
pJ201 mNeonGreen #1	Plasmid encoding mNeonGreen with codon optimized sequence for *S. aureus*, Kan^R	Pereira and Pinho, unpublished
pMAD_Plrg_mNeonGreen	Integrative pMAD derivative containing the up- and downstream regions of the *lrg* promoter with a P_{lrg}-*mneongreen*, Amp^R Ery^R	This study
pMAD_lrgB_rbs_mNeonGreen	Integrative pMAD derivative containing the up- and downstream regions of the *lrgB* and and an extra RBS of *lrg* operon before *mneongreen*, Amp^R Ery^R	This study
pMAD_Pfap_mNeonGreen	Integrative pMAD derivative containing the up- and downstream regions of the *fap* promoter with a P_{fap}-*mneongreen*, Amp^R Ery^R	This study
pEPSA::AS-020	pEPSA5 derivative with a xylose-inducible antisense RNA for *fabZ*, Amp^R Cm^R	[107]

[a] abbreviations: Amp^R – Ampicillin resistant; Cm^R – Chloramphenicol resistant; Em^R – Erythromycin resistant

Escherichia coli DC10B and DH5α were grown at 37 °C with aeration in Lysogeny Broth (LB-Miller, Sigma-Aldrich) or LB agar (LA-Miller, VWR) supplemented with ampicillin (100 μg.mL^{-1}, Apollo Scientific) or kanamycin (50 μg.mL^{-1}, Apollo Scientific) when necessary.

Unless mentioned otherwise, *S. aureus* strains were grown at 37 or 30 °C with aeration in tryptic soy broth (TSB, Difco) or on tryptic soy agar (TSA, Difco) supplemented with erythromycin (10 μg.mL^{-1}, Apollo Scientific), chloramphenicol (15 μg.mL^{-1}, Sigma-Aldrich), or 5-bromo-4-chloro-3-indolyl-beta-D-galactoside (100 μg.mL^{-1}, X-Gal, Apollo Scientific) as appropriate.

Culture growth was followed by monitoring the optical density at 600 nm (OD_{600nm}).

2.2. Molecular Cloning

2.2.1. DNA manipulation

Total DNA was purified from *S. aureus* cells grown overnight on TSA plates at 37 °C. Cells were collected and resuspended in 100 μL of 50 mM EDTA (VWR) containing lysostaphin 100 μg.mL^{-1} (Sigma-Aldrich) and RNase 200 μg.mL^{-1} (Sigma-Aldrich) and incubated at 37 °C for 30 min. 400 μL of 50 mM EDTA and 500 μL of Nuclei Lysis solution (Promega) were added and the samples incubated at 80 °C for 5 min. After cooling the samples to room temperature, 200 μL of Protein Precipitation Solution (Promega) were added, followed by a 10 min incubation on ice. After centrifugation (10 min at 16000 *g*), the supernatant was collected and the DNA was precipitated with isopropanol (VWR) and centrifuged again to pellet the DNA. The obtained pellet was washed with 500 μL of 70 % (v/v) ethanol and resuspended in sterile water. Plasmid DNA was purified from *E. coli* DC10B or DH5α cells using the Wizard® Plus SV Miniprep kit (Promega) according to manufacturer's instructions.

PCR amplifications were performed using Phusion High-Fidelity DNA polymerase (Thermo Fisher Scientific) following manufacturer's instructions. Primers used are listed in Table 2.2. PCR products and digested DNA fragments were purified using the Wizard® SV Gel and PCR Clean-Up System (Promega).

DNA ligations were performed using Gibson Assembly® Master Mix (New England Biolabs) according to manufacturer's instructions[108].

All constructed plasmids and strains were confirmed by DNA sequencing (GATC Biotech).

2.2.2. *E. coli* transformation

DC10B competent cells were prepared according to the Rubidium Chloride Protocol described in Sambrook 1989, and stored at -80 °C. Plasmids or Gibson Assembly reaction products were added to competent cells and kept on ice for 15 min. The transformation mixture was then incubated for 1 min at 42 °C to promote exogenous DNA incorporation, and for 5 min in ice. Cells were allowed to recover by adding 1 mL LB was added and the transformation mixture and incubating for 60 min at 37 °C with aeration, followed by plating in LA supplemented with ampicillin 100 μg.mL^{-1}.

2.2.3. *S. aureus* transformation and transduction

RN4220 competent cells were prepared as previously described[109]. Briefly, cells were grown at 37 °C with aeration until OD_{600nm} was 0.4-0.5 and then collected by centrifugation (1438 *g* for 15 min at 4 °C). The cell pellet was washed with an initial culture volume (V_i) of ice-cold filter-sterilized sucrose 0.5 M (Sigma-Aldrich), harvested and washed again in 1/2 V_i of sucrose 0.5 M. Cells were then incubated on ice for 15 min, resuspended in 1/100 V_i of sucrose 0.5 M and stored at -80 °C. For

transformation, 0.5 µg of purified plasmid DNA were added to RN4220 competent cells and incubated in ice for 5 min. Cells were electroporated (2.5 kV, 25 µF, 100 Ω) in a 0.2 cm electroporation cuvette (BioRad) using a Gene Pulser Xcell apparatus (BioRad). Electroporated cells were immediately resuspended in 1 mL of TSB, incubated at 37 °C with aeration for 1 h (or 2 h at 30 °C when using a thermosensitive plasmid), and plated on TSA supplemented with erythromycin 10 µg.mL^{-1}.

Transduction was performed using bacteriophage 80α as previously described[110]. In order to prepare phage lysates, cells from the donor strain were grown overnight on TSA plates supplemented with erythromycin, collected and resuspended in 1 mL of TSB supplemented with $CaCl_2$ 5 mM. Phage 80α was serially diluted to 10^{-7} in phage buffer ($MgSO_4$ 1 mM; $CaCl_2$ 4 mM; Tris-HCl 50 mM pH 7.8; NaCl 5.9 g.L^{-1} gelatin 1 g.L^{-1}). 10 µL of each phage dilution and 10 µL the cell suspension were mixed together and added to 3 mL of phage top agar (casamino acids 3 g.L^{-1}, Difco; yeast extract 3 g.L^{-1}, Difco; sodium chloride 5.9 g.L^{-1}, Sigma-Aldrich; agar 5 g.L^{-1}, Difco; pH 7.8), supplemented with 5 mM $CaCl_2$. The mixtures were poured onto phage bottom agar (phage top agar with 15 g.L^{-1} of agar) supplemented with 5 mM $CaCl_2$ and incubated overnight at 30 °C. The plates showing confluent lysis were selected and incubated with 4 mL of ice-cold phage buffer for 1 h at 4 °C. The top agar and phage buffer were collected and vortexed to disrupt the agar. Samples were kept for 1 h at 4 °C to allow phage release from the agar, and then centrifuged at 1,438 *g* for 15 min at 4 °C to sediment the top agar. The supernatant was collected and filtered through a 0.45 µm-pore diameter sterile filter (Sarstedt).

For the transduction, the receiving strain was grown overnight on TSA at 37 °C and resuspended in 1 mL TSB supplemented with 5 mM $CaCl_2$. Different volumes of phage lysate (1 µL, 10 µL and 100 µL) were mixed with 100 µL of cell suspension and phage buffer to a final volume of 300 µL. A control tube in which no phage lysate was added was also prepared. The transduction mixtures were incubated for 20 min at 37 °C and then added to 3 mL 0.3GL top agar (casamino acids 3 g.L^{-1}, Difco; yeast extract 3 g.L^{-1}, Difco; NaCl 5.9 g.L^{-1}, Sigma-Aldrich; sodium lactate 60 % syrup 3.3 mL.L^{-1}, Sigma-Aldrich; glycerol 50%, 2 mL.L^{-1}, Sigma-Aldrich; Tri-sodium citrate, 0.5 g.L^{-1}, Sigma-Aldrich; and agar 7.5 g.L^{-1}, Difco; pH 7.8). Transduction mixtures were poured onto plates containing a lower layer of 10 mL of 0.3GL bottom agar (0.3GL top agar with 15 g.L^{-1} agar) with 30 µg.mL^{-1} erythromycin and a top layer of 20 mL of 0.3GL bottom agar without antibiotics, prepared in the previous hour.

2.3. Construction of reporter *S. aureus* strains

To construct the *lrg* reporter strain with a transcriptional fusion of *mneongreen* to the *lrgAB* promoter (P_{lrg}), the regions upstream (1062 bp) and downstream (1078 bp) of the promoter were amplified separately, from *S. aureus* RN4220 (Table 2.1.) genomic DNA (followed by sequencing confirmation), using primers PlrgUpFwd/PlrgUpRev and PlrgDownFwd/PlrgDownRev (Table 2.2.), respectively. An alternative *lrg* reporter strain in which *mneongreen* was inserted at the end of the *lrgAB* operon was also constructed. The regions located immediately upstream (956 bp) and downstream (948 bp) of the stop codon of *lrgB* were amplified in two separate PCR reactions using primers lrg_mNeonGreen_Fwd/lrg_mNeonGreen_Rev and mNeonGreen_mngR_Fwd/ mNeonGreen_mngR_Rev, respectively. For the construction of the *fap* reporter strain with a transcriptional fusion of *mneongreen* to the *fapR* promoter (P_{fap}), the regions upstream (961 bp) and downstream (993 bp) of the promoter were amplified separately by PCR using primers PfapUpFwd/PfapUpRev and PfapDownFwd/PfapDownRev, respectively. For all constructions, a third PCR reaction was performed using pJ201 mNeonGreen #1 DNA as template and primers mNeonGreen_Fwd/mNeonGreen_Rev, resulting in a 712bp DNA fragment containing the mNeonGreen coding sequence. For each construct, the three amplification products were assembled together with

pMAD, previously linearized with FastDigest SmaI (Thermo Fisher Scientific) and dephosphorylated with FastAP Thermosensitive Alkaline Phosphatase (Thermo Fisher Scientific), using Gibson Assembly. The resulting plasmids (pMAD_Plrg_mNeonGreen, 12419 bp; pMAD_lrg_rbs_mNeonGreen, 12189 bp; pMAD_Pfap_mNeonGreen, 12224 bp) were introduced into RN4220 by electroporation and subsequently transduced into JE2. The insertion of the transcriptional reporters into the chromosome of *S. aureus* JE2 using the constructed pMAD-based vectors was performed according to the procedure described by Arnaud *et al*., 2004. Briefly, plasmids were integrated into the during a single recombination event, promoted by growth at a nonpermissive temperature for plasmid replication (43 °C). A second single recombination event during growth at a permissive temperature allowed reconstruction of the parental WT genotype or loss of the plasmid and the insertion of the reporter allele without introduction of antibiotic resistance determinants. The latter was identified by PCR using primers Plrg-mNeon_conf_fwd/Plrg-mNeon_conf_rev (for strain JE2_Plrg_mNeonGreen), lrg_mNeon_conf_Fwd/lrg_mNeon_conf_Rev (for strain JE2_lrgB_mNeonGreen) and Pfap-mNeon_conf_fwd/Pfap-mNeon_conf_rev (for strain JE2_Pfap_mNeonGreen), and also by sequencing.

Table 2.2. Primers used for construction of S. *aureus* reporter strains.

Primer name	Sequence (5'-3')
mNeonGreen_Fwd	ATGGTATCAAAAGGTGAAGAAGATAATATGG
mNeonGreen_Rev	TTATTTGTATAACTCATCCATGCCCATTAC
PlrgUpFwd	CTATCGATGCATGCCATGGTACCCCTGTAGAATCAGAGTCTGGAACTGG
PlrgUpRev	ATCTTCTTCACCTTTTGATACCATTGCCTCCTACGTTTGATTTAACTAAAG
PlrgDownFwd	GGCATGGATGAGTTATACAAATAAGAAAGATTTTAAAGCGTCGATAGG
PlrgDownRev	GAAGCTTCTAGAATTCGAGCTCCCTATACCACCGATACCAGCTGATAC
Plrg-mNeon_conf_fwd	GGTAACGATATTGACGTGTC
Plrg-mNeon_conf_rev	CTAATCCTCGGGCAATAGG
PfapUpFwd	CTATCGATGCATGCCATGGTACCCCTTGGGCAAAGCATGAGCAATACG
PfapUpRev	ATTATCTTCTTCACCTTTTGATACCATTTTTTAGTACCTAGTCTTAAACATTCC
PfapDownFwd	ATGGGCATGGATGAGTTATACAAATAAGCCATGCTGATTTGTCAATTTGAGTGC
PfapDownRev	GCAGAAGCTTCTAGAATTCGAGCTCCCTGTCTAAATTCGATTCGTTCATGG
Pfap-mNeon_conf_fwd	GTGTTATTTATGACAGCAACC
Pfap-mNeon_conf_rev	GACACACATCCATCTGCCTC
lrg_mNeonGreen_Fwd	CTATCGATGCATGCCATGGTACCCCAGCCGGTATCTCAGTTGTTAACTCTTTAGG
lrg_mNeonGreen_Rev	CACCTTTTGATACCATACACACCCTCCTACACACTTAGAAGAATATTGCTACAAAGAC
mNeonGreen_mngR_Fwd	TAATGGGCATGGATGAGTTATACAAATAAAACGAAAAACCTAAGCAAGATAATAGC
mNeonGreen_mngR_Rev	GCTTCTAGAATTCGAGCTCCCGTACCGGTTCAATTTGTAAACG
lrg_mNeon_conf_Fwd	TATGCCTGCATCAGTAATCG
lrg_mNeon_conf_Rev	CAGCTGTAAGAATGTCTTGG

For the construction of JE2 AS-*fabZ* and JE2_Pfap_mNeonGreen AS-*fabZ* strains, encoding an inducible antisense RNA targeting *fabZ*, the plasmid pEPSA::AS-020 was transduced into the WT and the *fap* reporter (JE2_Pfap_mNeonGreen) strains.

2.4. Determination of minimum inhibitory concentrations

MIC determination by microdilution in liquid medium was performed in sterile 96-well plates (Grenier Bio-One). Overnight cultures were diluted 1:1000 in Mueller Hinton broth (MHB, Quilaban) or TSB and 5 µL were inoculated in wells containing the following compounds, sequentially diluted two-fold in MHB or TSB: 0.125-64 $\mu g.mL^{-1}$ daptomycin (Cubist Pharmaceutical) in the presence of 50 $mg.L^{-1}$ of Ca^{2+} (according to CLSI 2015 guidelines), 0.125-64 $\mu g.mL^{-1}$ CCCP (Sigma-Aldrich), or 0.004-2 $\mu g.mL^{-1}$ triclosan (Merck). Plates were incubated at 37 °C without agitation and assessed for growth after 24 and 48 h. MICs were defined as the lowest concentration of compound at which visible growth was not observed. All MIC determinations were performed in triplicate.

2.5. Growth analysis of *S. aureus* strains

Growth curves of *S. aureus* strains were determined by measuring the OD_{600nm} of growing liquid cultures. Briefly, strains were grown overnight at 37 °C with aeration in MHB or TSB. Cultures were diluted to an initial OD_{600nm} of 0.05 in fresh medium, supplemented with $CaCl_2$ when required, and allowed to grow to mid-exponential phase ($OD_{600nm} \approx 0.4–0.5$). Daptomycin and CCCP were added at sub-MIC, MIC and supra-MIC conditions to cultures of *lrg* reporter strains, which were incubated for further 4 h. Triclosan was added at MIC and supra-MIC conditions to *fap* reporter strain, which was incubated for further 4 h.

2.6. *fabZ* antisense RNA induction

S. aureus JE2 (WT) and JE2_Pfap_mNeonGreen (harbouring the pEPSA5-based plasmid with the xylose-inducible antisense RNA for *fabZ*, pEPSA::AS-020) strains were grown overnight at 37 °C with aeration in TSB supplemented with chloramphenicol. Cultures were diluted to an initial OD_{600nm} of 0.05 in fresh TSB. Antisense induction was performed by adding 2% xylose (Sigma-Aldrich) to early-exponentially growing cultures ($OD_{600nm} \approx 0.09–0.10$) and incubating for further 3 h at 37 °C with aeration.

2.7. Fluorescence microscopy

Strains were grown overnight at 37 °C with aeration in MHB or TSB. Cultures were diluted to an initial OD_{600nm} of 0.05 in fresh MHB or TSB, supplemented with $CaCl_2$ when required, and allowed to grow until mid-exponential phase. Sub-, MIC and supra-MIC of triclosan, daptomycin and CCCP, 35 mM of glucose, 10 mM of potassium acetate and 100mM of sodium bicarbonate were added and the cultures incubated in the same conditions for further 3 h. Cells were pelleted by centrifugation (16000 *g*, 2 min), then washed and resuspended in phosphate-buffered saline (PBS) pH 7.4. Resuspended cells were mounted on microscope slides covered with a thin layer of 1.2 % agarose in PBS.

S. aureus DNA labelling was performed using Hoechst 33342 (Invitrogen). Prior to imaging, cells were incubated for 5 min with 1 $\mu g.mL^{-1}$ of Hoechst, in a ThermoMixer (Eppendorf) set at 37 °C and 800 rpm.

Fluorescence microscopy was performed using a Zeiss Axio Observer.Z1 microscope equipped with a Photometrics CoolSNAP HQ2 camera (Roper Scientific), using phase contrast objective Plan-

Apochromat 100 x/1.4 oil Ph3, with 0.24 µm resolution and 0.55 numerical aperture. The software used was black edition ZEN (Zeiss). Images of fluorescence microscopy were acquired using 1500 ms exposition time for mNeonGreen and 50 ms exposition time for Hoechst, when appropriate.

Analyses of microscopy images were performed using eHooke[111] and Fiji (http://imagej.net/Fiji).

2.8. Fluorimeter analysis

Strains were grown and cells collected as previously described for Fluorescence Microscopy. Fluorescence in each well of the black 96-well plates (BRANDplates® immunoGrade; Sigma-Aldrich) was then quantified using the FLUOstar OPTIMA microplate reader (excitation 485 nm and emission 520 nm; BMG Labtech) with 3 replicates per sample. As controls for autofluorescence and promoter-dependent mNeonGreen expression levels, WT and non-induced reporter strains were used, respectively. To determine the detection limit, JE2 WT parental strain was labelled with cell wall dye vancomycin conjugated to BODIPY™ FL (Van-FL, Invitrogen). Prior to imaging, cells were incubated for 5 min with a final concentration of 0.8 µg.mL^{-1} (1x) for Van-FL, in a ThermoMixer (Eppendorf) set at 37 °C and 800 rpm[112].

2.9. Statistical analysis

Statistical analyses were done using GraphPad Prism 6 (GraphPad Software). After eHooke quantifications, independent sample/unpaired Student's t-tests with Welch's correction (or Welch t-test) were used to compare mean of cells fluorescence between the positive control and the different induction conditions for each reporter strain. Therefore, Welch t-test defined whether the fluorescent inducible response was a significant difference[113].

Fluorescence data from the fluorimeter analysis was compared after calculations of mean, median and standard deviation (SD).

3. Results

3.1. Construction of mNeonGreen reporter strains

To analyse the promoter activity of the *lrg* operon and *fap* regulon in the presence of compounds known to decrease bacterial cell membrane potential or to prevent lipid synthesis, respectively, promoter sequences were fused to a gene encoding the green fluorescent protein mNeonGreen[114]. These constructs were inserted adjacently to the native *S. aureus* chromosomal *locus* for each promoter (Figure 3.1.A and Figure 3.1.C), which allowed the native operons to remain intact while monitoring promoter activity. Since this led to a duplication of the promoter region, an alternative strategy for the *lrg* reporter was also used, in which the gene encoding mNeonGreen was inserted at the end of the *lrgAB* operon (Figure 3.1.B), thus being co-transcribed with the *lrg* genes as a single polycistronic unit. The RBS of *lrgA* and fapR (same sequence and spacing to the start codon) were used for *mneongreen* translation in JE2_Plrg_mNeonGreen and JE2_Pfap_mNeonGreen strains, respectively.

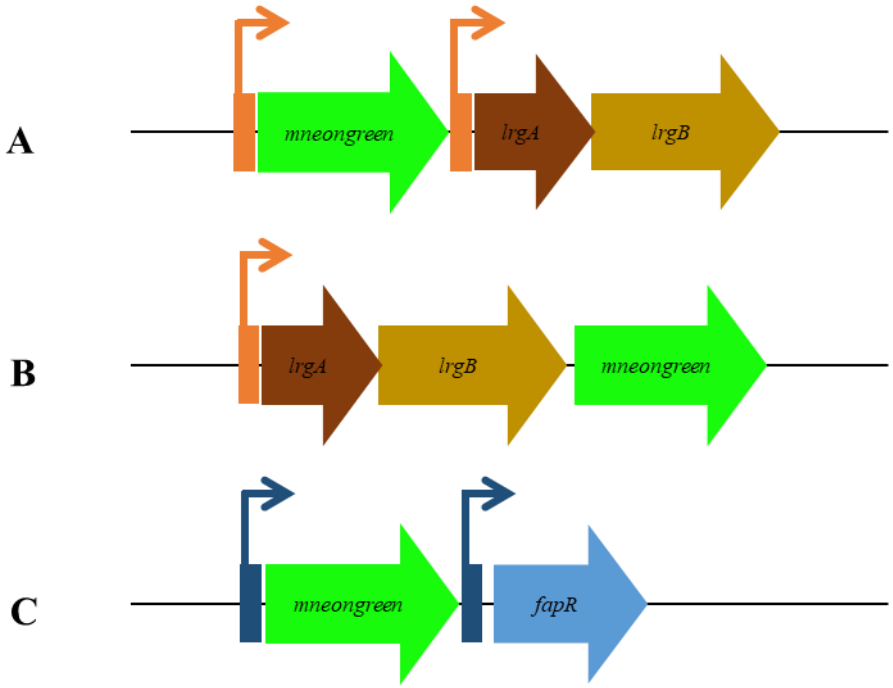

Figure 3.1. Schematic representation of the chromosomal organization of strains expressing different promoter fusions. Integration of the different constructs into the native *locus* resulted in a duplication of promoter sequences in A and C. The activity of the different promoters can be followed while maintaining the integrity of the native operons: A – P_{lrg} promoter fusion to *mneongreen*, B – expression of *mneongreen* from the *lrg* operon, C – P_{fap} promoter fusion to *mneongreen*.

To check if the genetic constructs introduced in the *lrg* and *fap* regions affected susceptibility to compounds that trigger expression of these operons, we tested if the reporter strains displayed a similar susceptibility phenotype to CCCP and daptomycin (which activate the *lrg* reporters), and triclosan (which inhibit lipid biosynthesis and activate the *fap* reporter) as the WT parental strain. For that purpose, MICs were determined (Table 3.1.).

According to the results presented in Table 3.1., the insertion of the fluorescence reporters in the chromosome of JE2 did not significantly impact the MICs, when compared with WT JE2 strain, to the tested compounds. MICs were also determined in TSB (Supplementary Table 1) and the results were comparable with those obtained using MHB.

Table 3.1. MICs of reporter strains to compounds that affect membrane potential or fatty acid biosynthesis. The MIC of each compound was determined by microdilution method in MHB and values were obtained based on the average of three independent experiments.

Strain	CCCP MIC (µg.mL^{-1})	Daptomycin[b] MIC (µg.mL^{-1})	Triclosan MIC (µg.mL^{-1}; 24 h)	Triclosan MIC (µg.mL^{-1}; 48 h)
JE2	1	1	7.8×10^{-3}	6.25×10^{-2}
JE2_Plrg_mNeonGreen	1	1		
JE2_lrgB_mNeonGreen	1	1		
JE2_Pfap_mNeonGreen			7.8×10^{-3}	6.25×10^{-2}

[b]MICs determined in: MHB supplemented with 50 mg.L^{-1} of Ca^{2+} (Ca-MHB)

To find the best conditions to test the previously mentioned compounds, the reporter strains were grown in liquid MHB with aeration, and different concentrations of the compounds used for MIC determination were added after cultures reached the mid-exponential phase (Figures 3.2. and 3.3.).

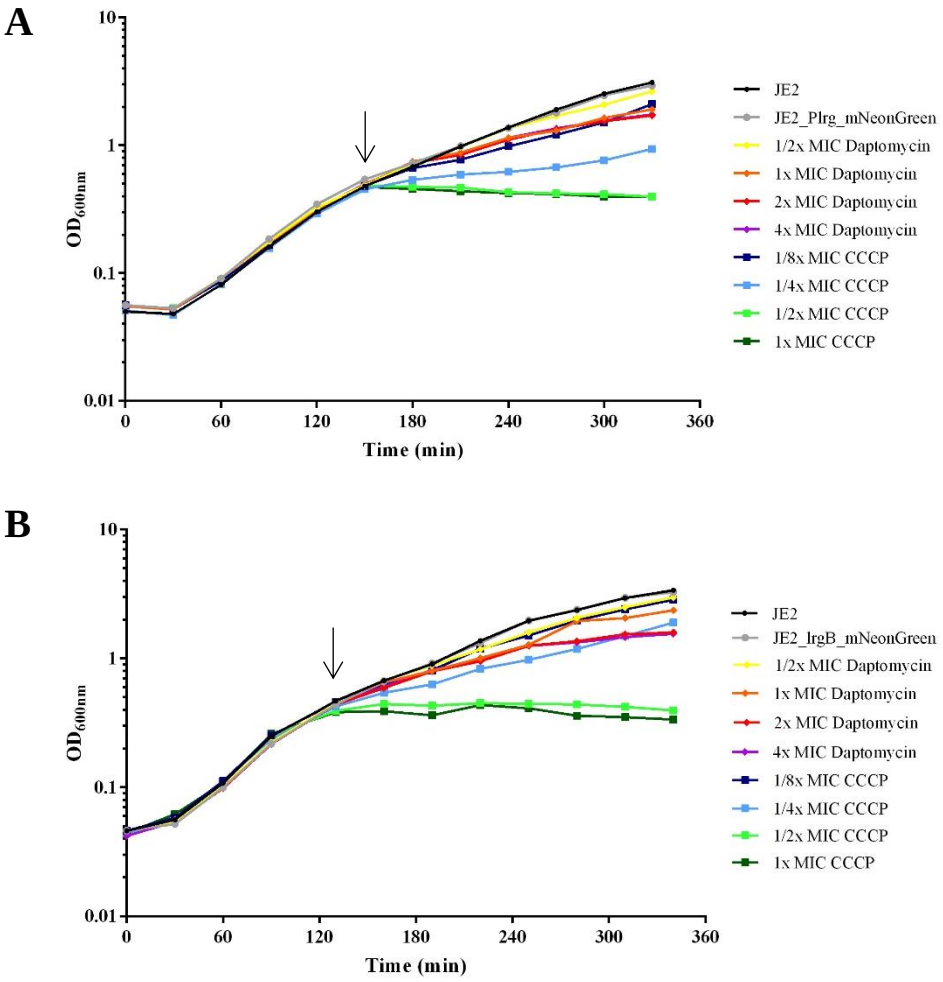

Figure 3.2. Growth curves of *lrg* reporter strains. Cultures from JE2_Plrg_mNeonGreen and JE2_lrgB_mNeonGreen were grown overnight in MHB at 37 °C and re-inoculated in fresh MHB, supplemented with 50 mg.L^{-1} $CaCl_2$ for daptomycin. Both figures A and B show growth curves obtained through regular measurements of optical density at 600 nm. Time of induction with appropriate concentration of either daptomycin or CCCP is indicated by the black arrow. Addition of sub MIC concentrations of CCCP, significantly slowed bacterial growth of P_{lrg} promoter fusion to *mneongreen* (A) and *lrg* fusion to *mneongreen* (B) reporter strains, while daptomycin has a milder effect.

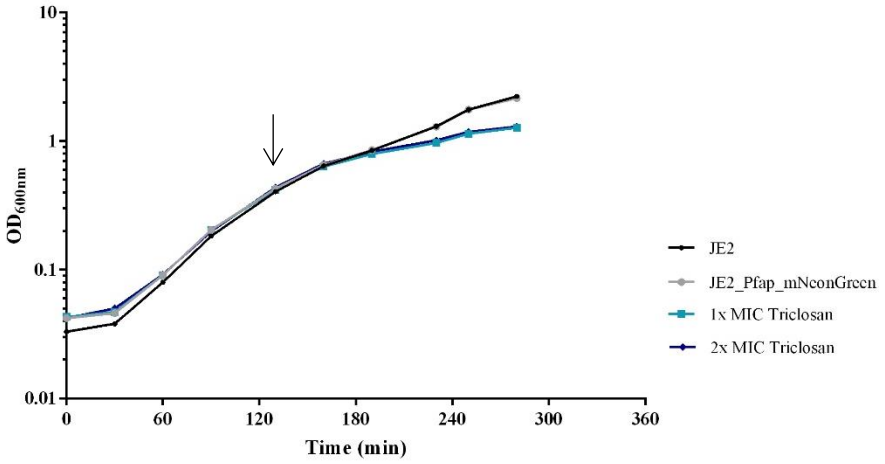

Figure 3.3. Growth curves of P_{fap} reporter strain. Cultures from JE2_Pfap_mNeonGreen were grown overnight in MHB at 37 °C, re-inoculated in fresh media and regular measurements of optical density at 600 nm were made. Time of induction with appropriate concentration of triclosan is indicated by the black arrow.

For all three reporter strains, growth profiles in the absence of inducers are similar to that of the WT strain, confirming that the fluorescent reporter alleles have no impact in fitness in the conditions tested. As expected, growth slows down upon addition of daptomycin, CCCP or triclosan to growing cultures. CCCP has a faster and stronger effect on *lrg* reporter strains than daptomycin at any concentration tested (Figure 3.2.). For the *fap* reporter strain, a noticeable decrease in the growth rate is observed 1 h after addition of triclosan (Figure 3.3.). Growth curves were also determined for this reporter strains in TSB and the results were comparable with those obtained using MHB (Supplementary Figure 1).

Therefore, the set of constructed strains (Figure 3.1.) was deemed suitable to monitor the activity of P_{lrg} and P_{fap} in response to the presence of compounds by measuring total fluorescence of individual cells using fluorescence microscopy.

3.2. Induction of *lrg* reporter

To further assess the best conditions to test the response of the transcriptional fusion of *mneongreen* to the promoter of *lrgAB* to the dissipation of membrane potential, growing cultures of the JE2_Plrg_mNeonGreen strain were challenged with 0.25x, 1x and 4x MIC of daptomycin (Figure 3.4.) or CCCP (Figure 3.5.). Cells were imaged at different times of induction and microscopy images were used to quantify total average fluorescence of individual cells in a sample. The obtained results are depicted in Figure 3.6.

Changes in total fluorescence levels from P_{lrg}-dependent mNeonGreen expression in the presence of daptomycin were only observed when cells were challenged for longer periods with supra-MIC antibiotic concentrations. Moreover, the measured activity of the *lrg* promoter in the presence of daptomycin is highly heterogeneous between cells of the same sample (Figure 3.6.). In addition, the presence of higher concentrations of daptomycin led to cell enlargement (Figure 3.4.). Similarly, CCCP-challenged cells display a slightly increased fluorescence signal when compound concentrations are used above the determined MIC and for longer incubation periods (Figure 3.6.E and 3.6.F). In contrast with the results obtained with daptomycin, the *lrg* system response to the presence of CCCP is less heterogeneous. P_{lrg} activation was also tested in the same conditions using TSB as growth media and results were comparable with those obtained when using MHB (data not shown).

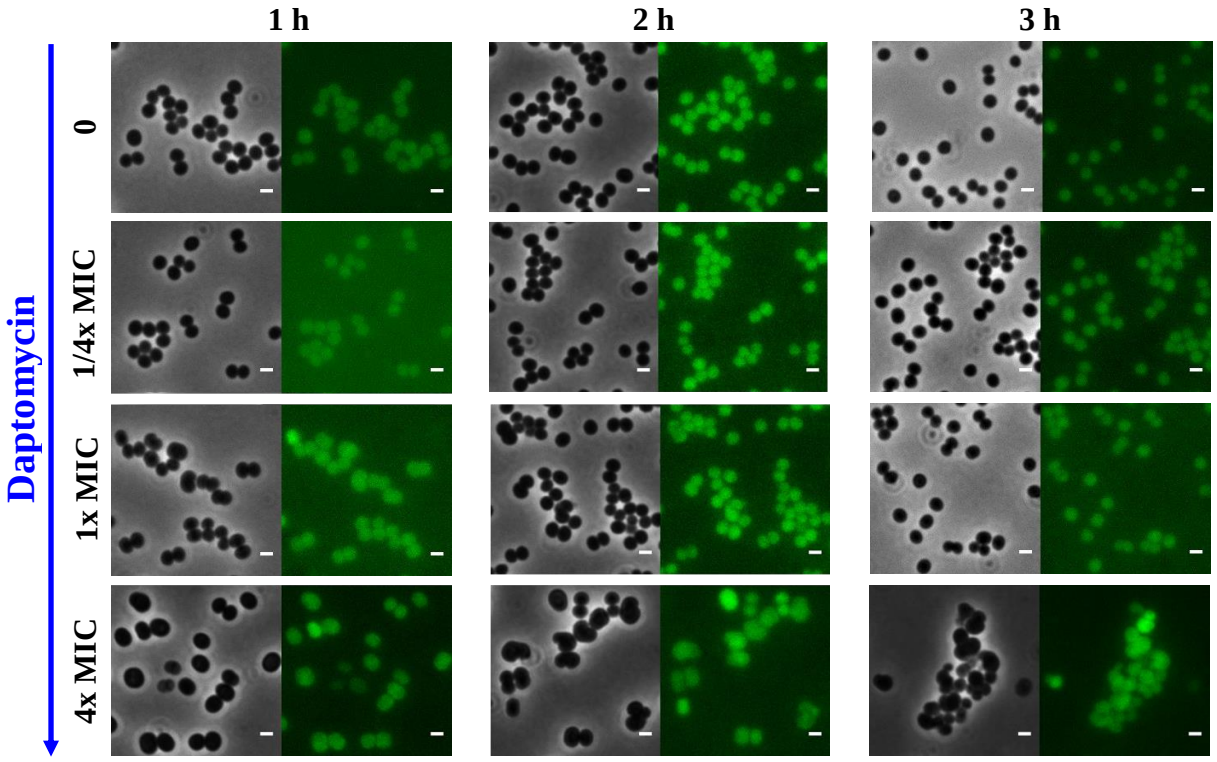

Figure 3.4. Microscopy images of JE2_Plrg_mNeonGreen exposed to daptomycin. JE2 reporter cells expressing mNeonGreen under the control of P_{lrg} promoter without daptomycin, with 0.25x, 1x and 4x MIC of daptomycin. Each two-panels show cells at 1 h, 2 h and 3 h of incubation/induction with daptomycin. For each two-panel example: left – phase contrast image; right – GFP filter image. Scale bars = 1 μm.

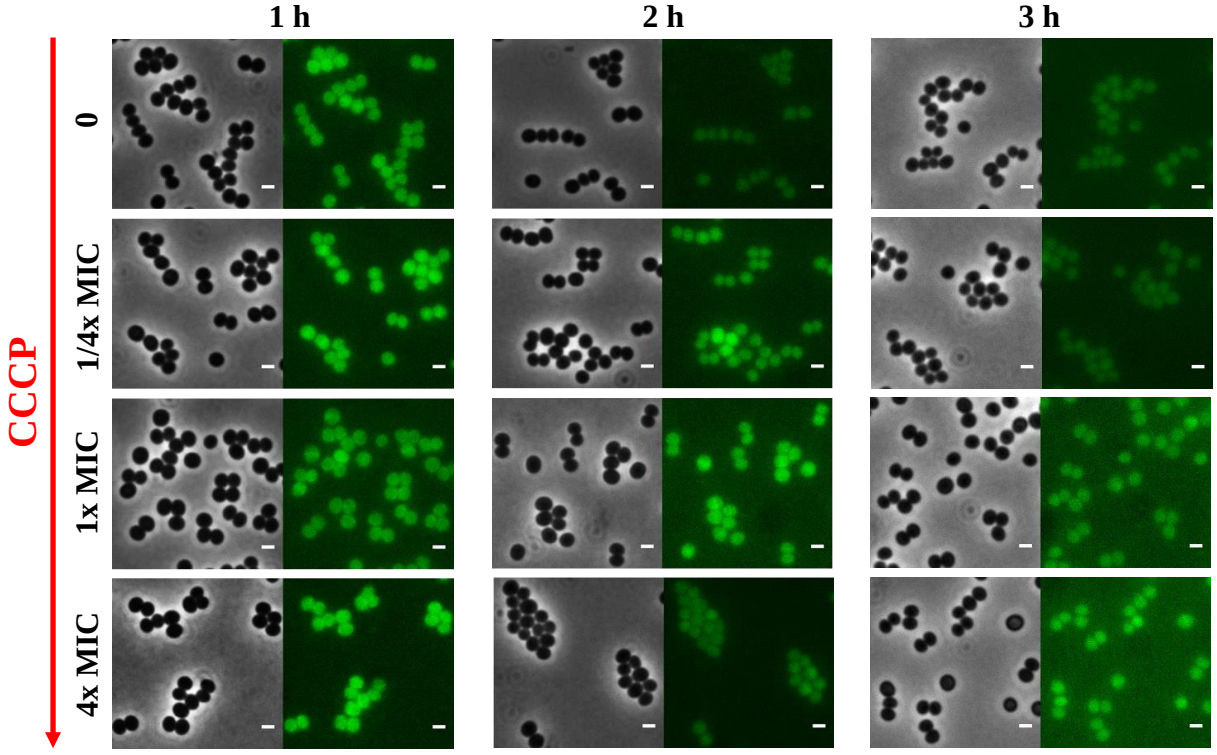

Figure 3.5. Microscopy images of JE2_Plrg_mNeonGreen exposed to CCCP. JE2 reporter cells expressing mNeonGreen under the control of P_{lrg} promoter without CCCP, with 0.25x, 1x and 4x MIC of daptomycin. Each two-panels show cells at 1 h, 2 h and 3 h of incubation/induction with daptomycin. For each two-panel example: left – phase contrast image; right – GFP filter image. Scale bars = 1 μm.

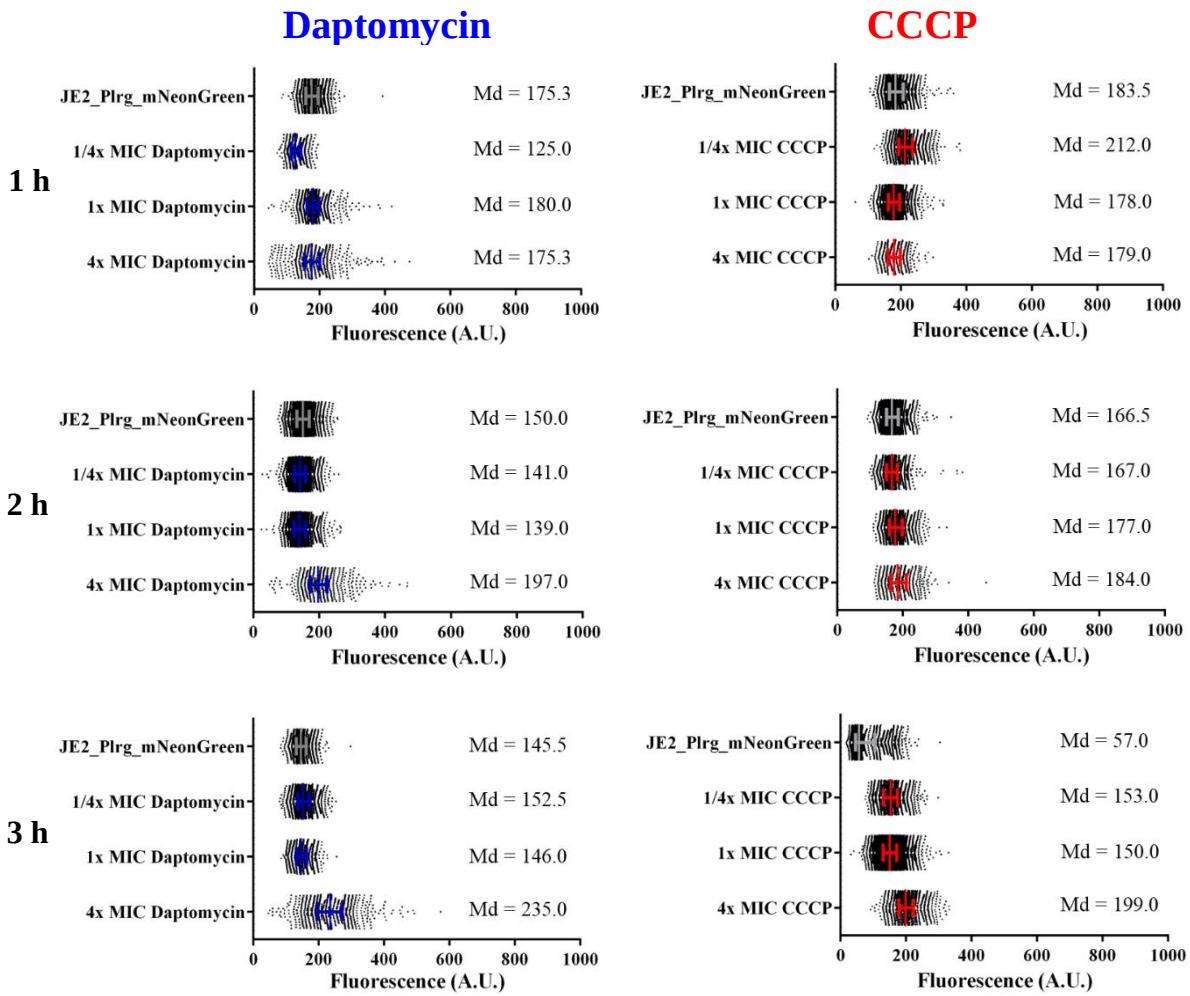

Figure 3.6. P_{lrg} promoter activity in the absence or presence of daptomycin and CCCP. JE2 reporter cells challenged with 0.25x, 1x and 4x MIC of daptomycin induction as well as with 0.25x, 1x and 4x MIC of CCCP, during 1 h, 2 h and 3 h. N=500 cells were analysed for each condition tested. Each quantified cell is represented by a dot in the graphics. Grey lines, blue lines and red lines represent median (Md) with interquartile range for samples with non-induced cells, daptomycin and CCCP-challenged cells, respectively. The median value for each tested condition is indicated.

To sum up, microscopy assays indicate an heterogenous and inconsistent activation of the P_{lrg} reporter strain by daptomycin and weak activation of the system by CCCP.

In order to assess whether the activation of P_{lrg} could be triggered through a different approach, the accumulation of acetate in the presence of excess glucose was also tested[115]. Additionally, the effect of sodium bicarbonate[116] in the activation of the *lrg* response system by altering the membrane potential was assessed (Figure 3.7.).

The data presented in Figure 3.7. indicate that the fluorescence levels of induced cells did not increase in any of the conditions tested. Interestingly, fluorescence is lower in the presence of glucose suggesting that it is apparently leading to repression of the *lrg* response system. After 2 h of induction with potassium acetate, the fluorescence of challenged cells also decreased. However, at 1 h and 3 h of induction this effect was not observed. Using this approach, P_{lrg} activation was also tested in the same conditions using TSB as growth media and results were comparable with those obtained when using MHB (data not shown).

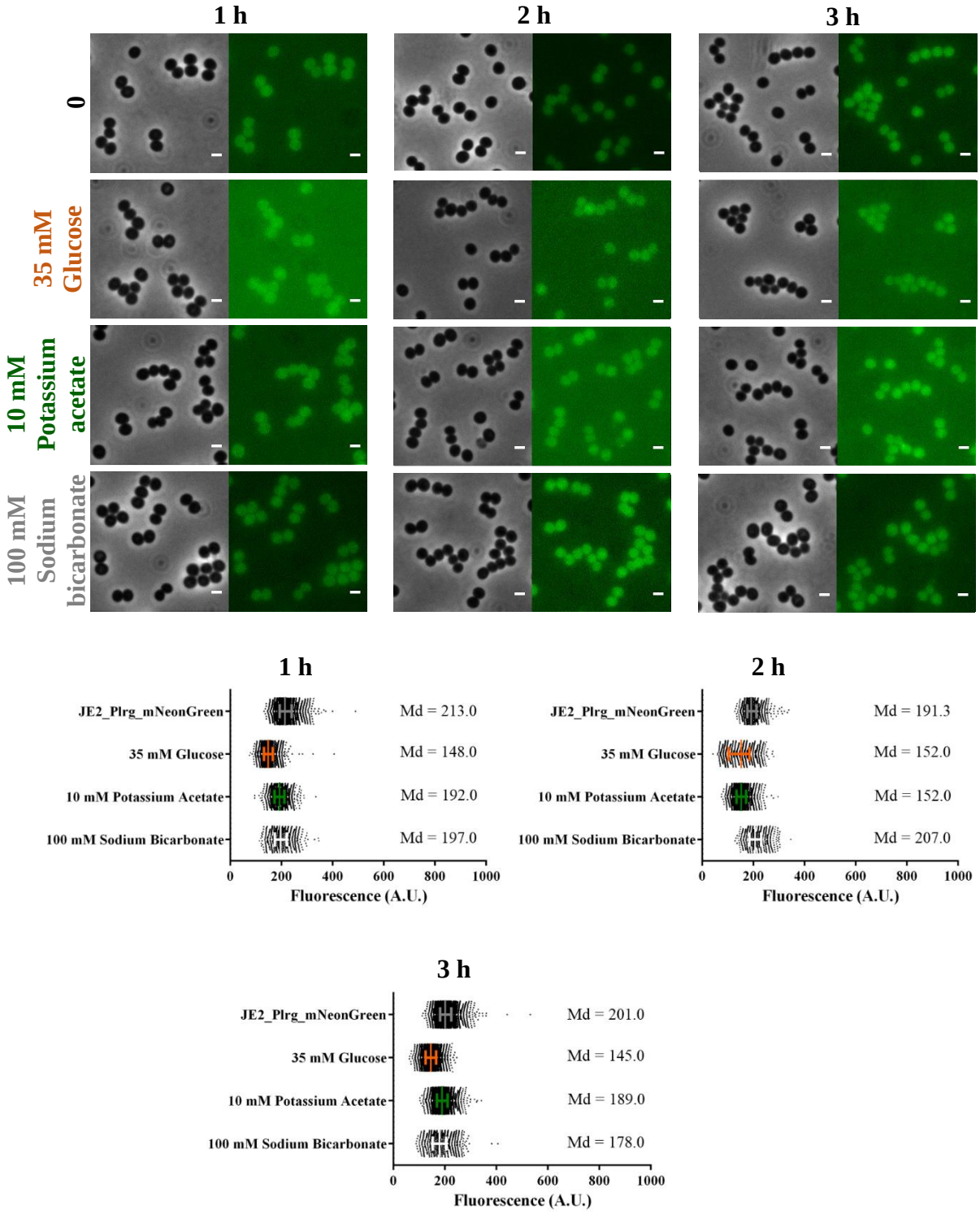

Figure 3.7. Microscopy images and quantification of P_{lrg} promoter activity of JE2_Plrg_mNeonGreen exposed to glucose, acetate and bicarbonate. JE2 reporter cells expressing mNeonGreen under the control of P_{lrg} promoter without inducer, with 35 mM glucose[115], 10 mM potassium acetate and 100 mM sodium bicarbonate ([116] supplementary data). Each two-panels show cells at 1 h, 2 h and 3 h of incubation with the appropriate inducer. For each two-panel example: left – phase contrast image; right – GFP filter image. Scale bars = 1 µm. P_{lrg} promoter activity was measured by quantification of total average fluorescence of individual cells in a sample in the conditions previously mentioned are shown at 1 h, 2 h and 3 h of induction. N=500 cells were analysed for each condition tested. Each quantified cell is represented by a dot in the graphics. Grey, orange, green and white lines represent median (Md) with interquartile range for samples with non-induced cells, glucose, acetate and bicarbonate-challenged cells, respectively. The median value for each tested condition is indicated.

3.3. Alternative *lrg* reporter

As described above, despite having tested several approaches to activate this P_{lrg} reporter strain, low induction of mNeonGreen expression was always observed. We reasoned that one possible explanation was the duplication of the promoter, present in this strain, led to a titration of the available molecules of activator LyR/promoter. We therefore constructed a new strain, JE2_lrg_mNeonGreen, where the *mneongreen* reporter gene was placed as the last gene of the *lrgAB* operon, thus avoiding the duplication of the promoter. The response of this new reporter strain to membrane potential decrease, caused by the presence of daptomycin (Figure 3.8.) and CCCP (Figure 3.9.), was then assessed. Cells were imaged after 1 h and 2 h of induction.

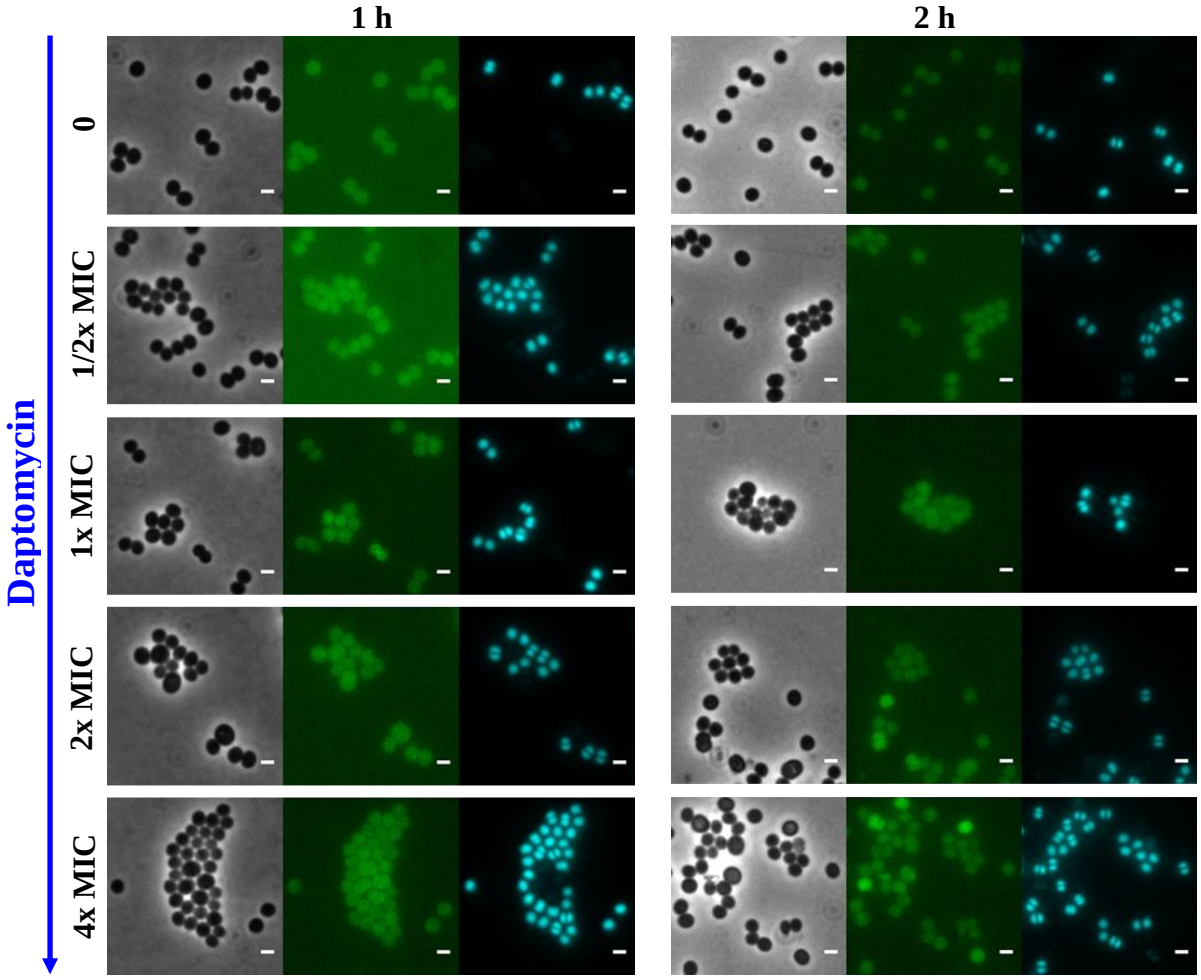

Figure 3.8. Microscopy images of JE2_lrgB_mNeonGreen exposed to daptomycin. JE2 reporter cells expressing mNeonGreen under the control of P_{lrg} promoter without inducer, with 0.5x, 1x, 2x and 4x MIC of daptomycin. In every condition tested, non-induced cells were labelled with DNA dye Hoechst 33342 and then mixed with cells non-challenged or challenged by daptomycin, as appropriate. Each three-panels show cells at 1 h and 2 h of incubation with the appropriate concentration of daptomycin/inducer. For each three-panel example: left – phase contrast image; middle – GFP filter image; right – DAPI filter image. Scale bars = 1 μm.

In order to obtain measurements of the fluorescence levels more comparable between different conditions, a culture of non-induced cells was used as internal control in every experiment. These cells were labelled with DNA dye Hoechst 33342 and then mixed with cells challenged by daptomycin or CCCP. This allowed the identification of induced and non-induced cells and the quantification of their total fluorescence separately (Figure 3.10.), after which the ratio between the two values of median was

calculated. The reverse experiment was also performed to assess whether this additional staining had any effect on mNeonGreen expression. Quantification of these results allowed us to conclude that the DNA dye did not alter fluorescence of mNeonGreen in challenged cells (data not shown).

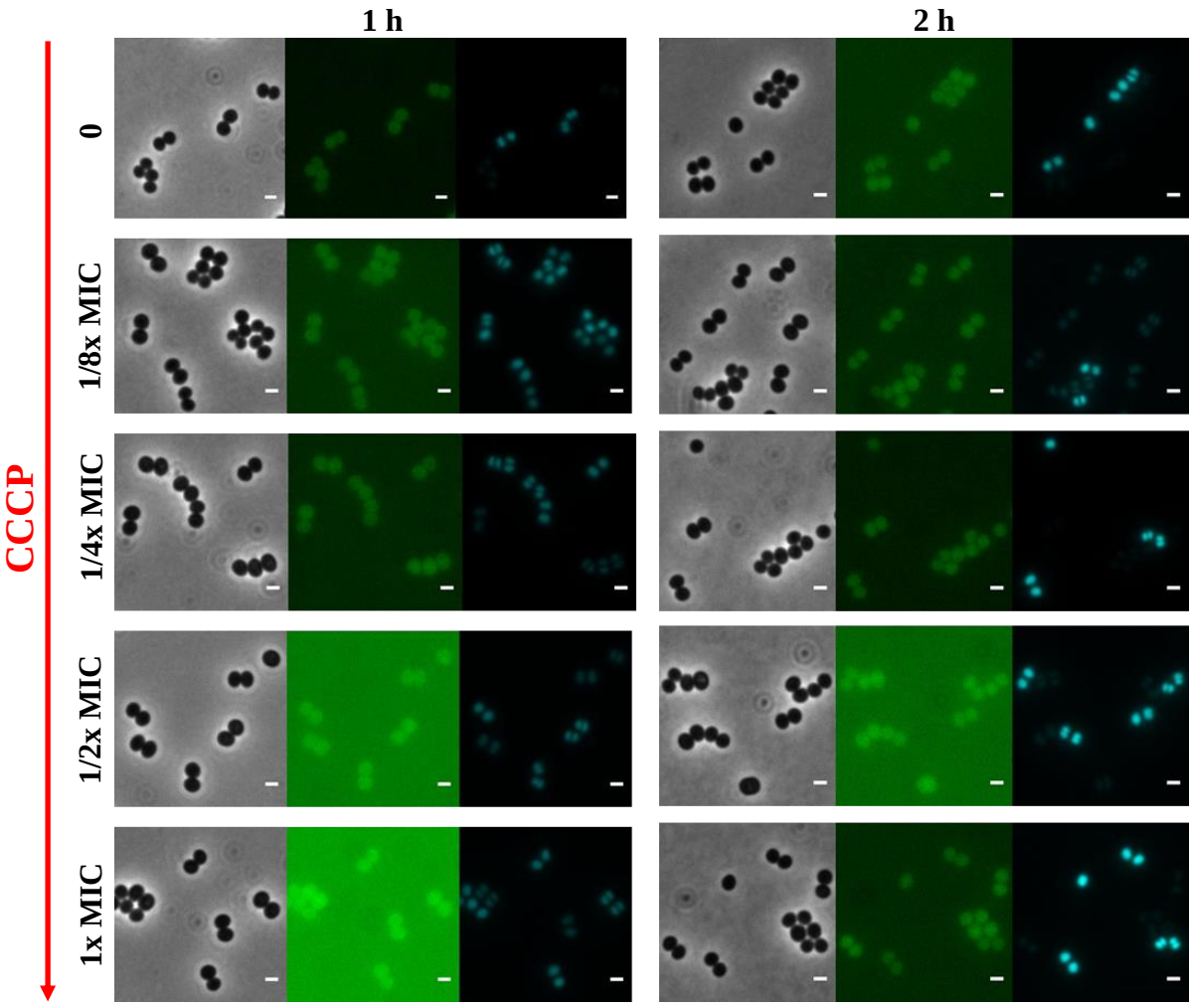

Figure 3.9. Microscopy images of JE2_lrgB_mNeonGreen exposed to CCCP. JE2 reporter cells expressing mNeonGreen under the control of P_{lrg} promoter without inducer, with 0.125x, 0.25x, 0.5x and 1x MIC of CCCP. In every condition tested, non-induced cells were labelled with DNA dye Hoechst 33342 and then mixed with cells non-challenged or challenged by daptomycin, as appropriate. Each three-panels show cells at 1 h and 2 h of incubation with the appropriate concentration of CCCP/inducer. For each three-panel example: left – phase contrast image; middle – GFP filter image; right – DAPI filter image. Scale bars = 1 μm.

Similarly to the results obtained for strain JE2_Plrg_mNeonGreen, induction of mNeonGreen expression in the presence of daptomycin was heterogeneous, and comparable only when using an antibiotic concentration above the MIC (Figure 3.10.). For this alternative strain, a sub-MIC concentration of CCCP was sufficient to activate the response of the *lrg* system and, consequently, to increase the total fluorescence of cells challenged by the uncoupler agent (Figure 3.10.). Identical results were obtained from mixing non-induced with DAPI-stained induced-cells (data not shown). However, this improvement in the fluorescence results of the *lrg* reporter strain is, however, insufficient for this strain to be used as a tool in future HTS.

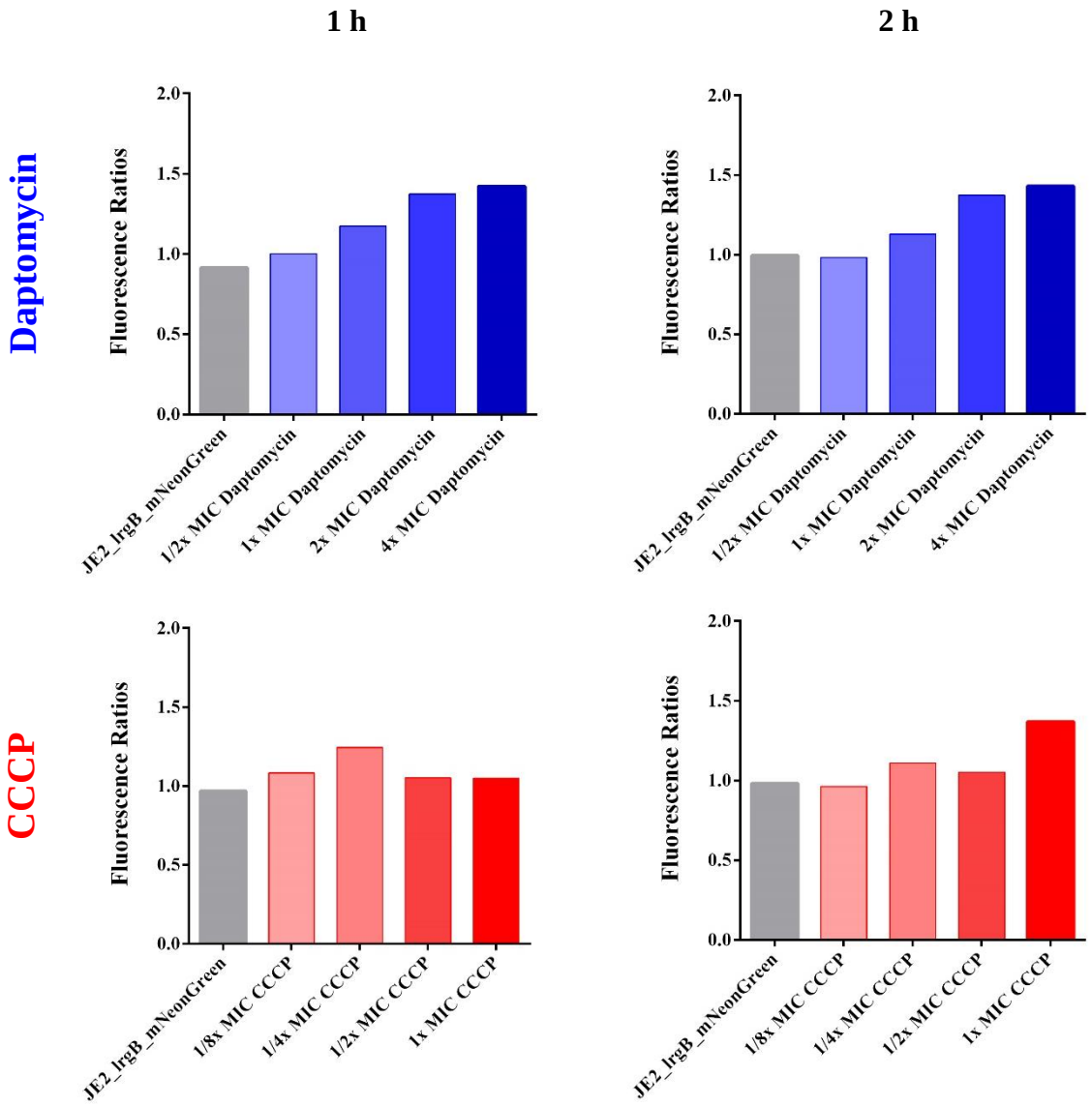

Figure 3.10. Promoter activity of *lrgB* fusion to *mneongreen* in the absence or presence of daptomycin and CCCP through quantification of mNeonGreen fluorescence. JE2 reporter cells were challenged with 0.5x, 1x, 2x and 4x MIC of daptomycin induction as well as with 0.125x, 0.25x, 0.5x and 1x MIC of CCCP equally during 1 h and 2 h. Bars represent the calculated ratio of the medians between daptomycin or CCCP induced cells and non-induced but DNA-labelled cells. N=500 cells were analysed for each condition tested. Blue and red lines indicate de increase of fluorescence ratios compared to the JE2_Pfap_mNeonGreen control, due to daptomycin and CCCP induction, respectively.

3.4. Induction of *fap* reporter

To test the transcriptional fusion of *mneongreen* to the promoter of *fapR* and the cellular response of the constructed reporter to FapR de-repression, growing cultures of strain JE2_Pfap_mNeonGreen were challenged with 1x and 2x MIC (Table 3.1.) for triclosan (Figure 3.11). The DNA labelling process was also performed during assays with the P_{fap} reporter strain. DNA labelling allowed identification of induced and non-induced cells and subsequent quantification of total fluorescence, used for calculating ratios of median fluorescence (Figure 3.12.).

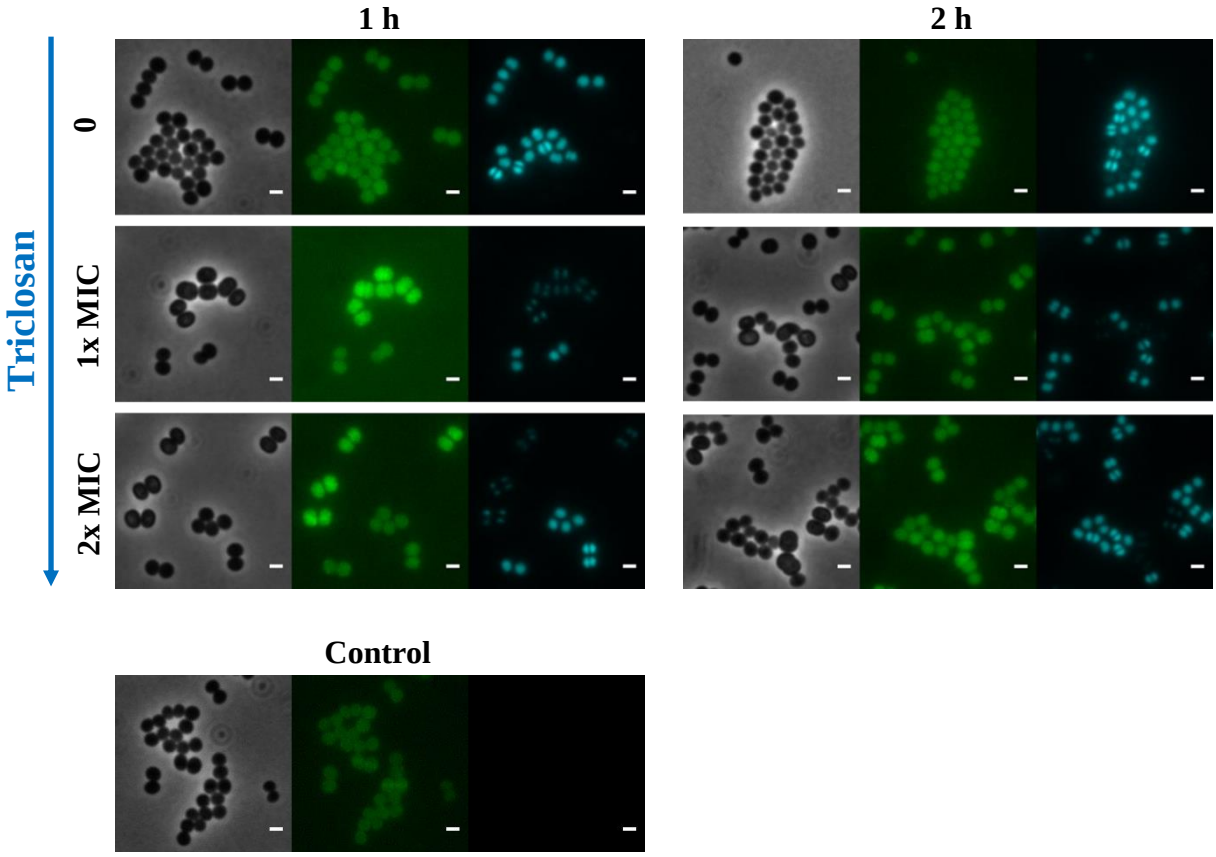

Figure 3.11. Microscopy images of JE2_Pfap_mNeonGreen exposed to triclosan. JE2 reporter cells expressing mNeonGreen under the control of P_{fap} promoter without inducer, with 1x and 2x MIC of triclosan (in TSB). In every condition tested, non-induced cells were labelled with DNA dye Hoechst and then mixed with cells non-challenged or challenged by daptomycin, as appropriate. Each three-panels show cells at 1 h and 2 h of incubation with the appropriate concentration of triclosan/inducer. As a control, WT parental cells were mixed with triclosan and imaged. For each three-panel example: left – phase contrast image; middle – GFP filter image; right – DAPI filter image. Scale bars = 1 µm.

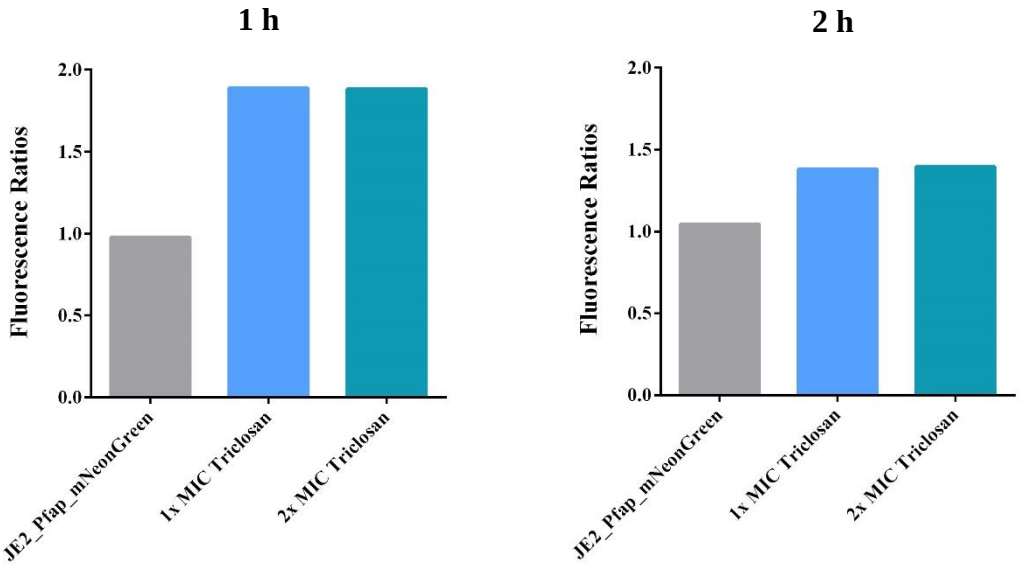

Figure 3.12. P_{fap} promoter activity in the absence or presence of triclosan through quantification of mNeonGreen fluorescence. JE2 reporter cells were previously challenged with 1x and 2x MIC of triclosan induction for 1 h and 2 h. Bars represent the calculated ratio of the medians between triclosan induced cells and non-induced but DNA-labelled cells. N=500 cells were analysed for each condition tested. Coloured lines indicate de increase of fluorescence ratios compared to the JE2_Pfap_mNeonGreen control.

Increase in total fluorescence levels (data not shown) was reflected in higher fluorescence ratios regarding P_{fap}-dependent mNeonGreen expression in the presence of triclosan. This increase was immediately observed when cells were challenged for 1 h with MIC or supra-MIC antibiotic concentrations, and it corresponds to almost a two-fold change in mNeonGreen fluorescence intensity (Figure 3.12.). The presence of higher concentrations of triclosan led to cell enlargement (Figure 3.11.), which was also already noticeable at 1 h with MIC conditions (Figure 3.11.A). Identical results were obtained from mixing non-induced with DAPI-stained induced-cells (data not shown). Contrary to the previous reporter strains, P_{fap} activation was only tested using TSB as growth media.

To further validate the *fap* reporter strain, a different approach was taken by targeting *fabZ* with an RNA antisense system (Figure 3.13.). This leads to the inhibition of one of the elongation steps of the fatty acid biosynthesis, which subsequently results in the increase of malonyl-CoA concentration inside the cell, followed de-repression and expression of the *fap* regulon[91,93]. Similarly to the previous approach, microscopy assays (Figure 3.13.) were just performed using cultures grown in TSB.

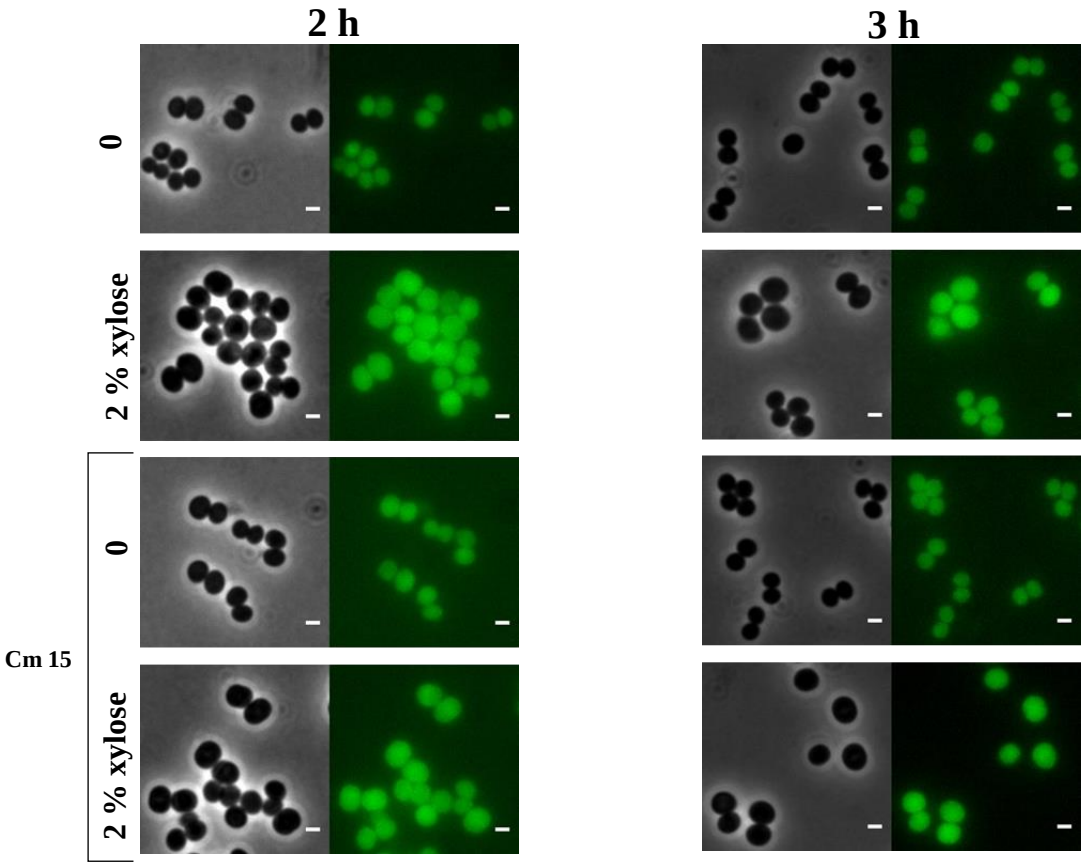

Figure 3.13. Microscopy images of *fabZ* RNA antisense induction of *fap* reporter strain. JE2_Pfap_mNeonGreen AS-*fabZ* expressing mNeonGreen under the control of P_{fap} promoter without xylose-induction, with 2% xylose, without xylose-induction but in the presence of 15 µg.mL^{-1} of chloramphenicol (Cm15) and with 2% xylose and chloramphenicol (in TSB). Cm15 was added in half of the cultures as a selective pressure control for plasmid with a xylose inducible antisense RNA for *fabZ*. Each two-panels show cells at 2 h and 3 h of induction. For each two-panel example: left – phase contrast image; right – GFP filter image. Scale bars = 1 µm.

Microscopy images were used to quantify total average fluorescence of individual cells in a sample in the conditions tested. The obtained results are depicted in Figure 3.14.

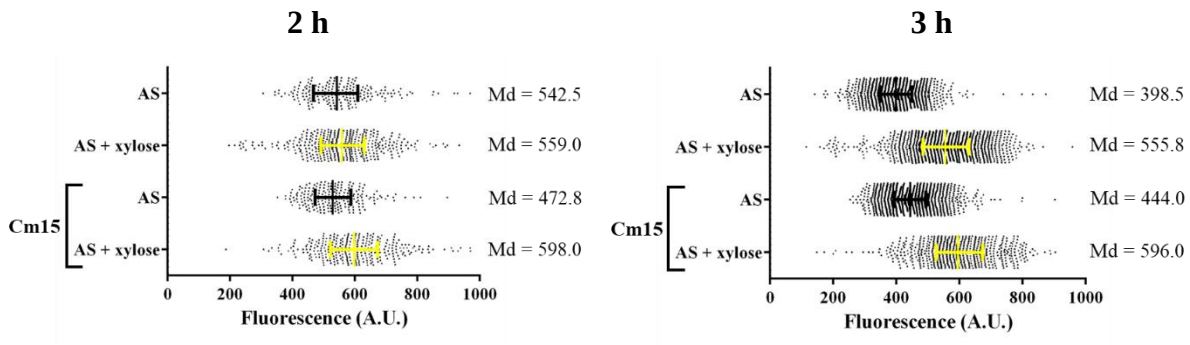

Figure 3.14. P_{fap} promoter activity upon induction of *fabZ* antisense RNA and fluorescence from mNeonGreen expression was quantified. JE2 reporter cells were challenge with 2% of xylose, in the absence or in the presence of 15 µg.mL^{-1} of chloramphenicol (Cm15), for 2 h and 3 h of induction. Cm15 was added in half of the cultures as a selective pressure control for plasmid with a xylose inducible antisense RNA for *fabZ*. N=500 cells were analysed for each condition tested. Each quantified cell is represented by a dot in the graphics. Black and yellow lines represent median (Md) with interquartile range for samples with non-induced cells and triclosan-challenged cells, respectively. The median value for each tested condition was added.

Data presented in Figure 3.14. shows that a 2 h induction period with xylose does not result in significant changes in fluorescence levels, even though cell enlargement is already noticeable (Figure 3.13.). However, fluorescence levels of induced cells increased after 3 h of xylose-induction, indicating a significant upregulation of the *fap* genes.

Considering all previous results, the *fap* reporter strain was deemed the most suitable tool, constructed in this work, for a future HTS.

3.5. Initial optimization for subsequent high-throughput screening

Since microscopy studies are not compatible with HTS of large libraries of compounds, we chose to perform an initial test on a fluorimeter microplate system. By maintaining the same tested conditions (1 h and 2 h of induction with 1x and 2x MIC of triclosan) for the strain with the transcriptional fusion of *mneongreen* to the promoter of *fapR*, cultures of JE2_Pfap_mNeonGreen and JE2 WT were grown and then inoculated in microplates as detailed in Materials and Methods. For this set of experiments the $OD_{600\ nm}$ was adjusted to 0.1 in PBS, to prevent background autofluorescence, and measurements were performed in black 96-well microplates, to avoid light scattering.

Data obtained from fluorimeter assays (Figure 3.15.) was non-reproducible and did not correlate with the previously observed two-fold increment in mNeonGreen fluorescence ratio (Figure 3.12.). Moreover, fluorescence of triclosan-challenged cells was inferior to the positive control of vancomycin-labelled cells at any tested concentration. Therefore, detection of the *fap* reporter fluorescence using a fluorimeter requires further optimization studies.

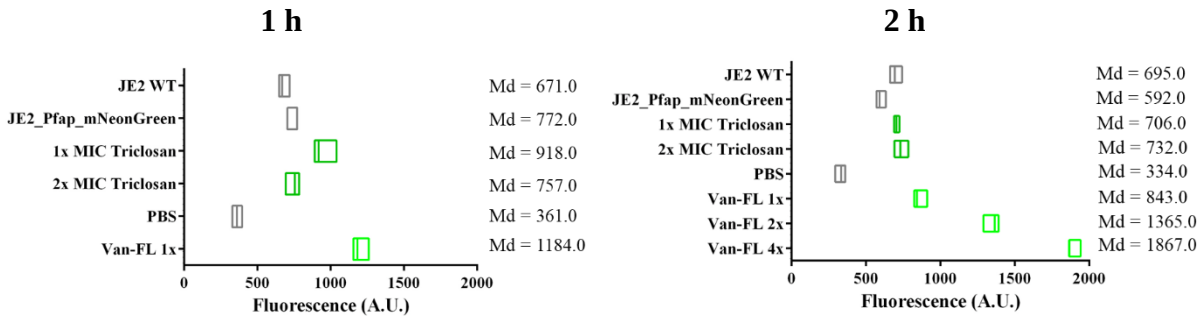

Figure 3.15. Quantification of mNeonGreen fluorescence levels of JE2_Pfap_mNeonGreen in the absence or presence of triclosan using a fluorimeter microplate system. JE2 WT strain and non-induced *fap* reporter cells represent controls for autofluorescence and basal promoter-dependent mNeonGreen expression levels, respectively. JE2 cells labelled with 0.8 µg.mL^{-1} (1x), 1.6 µg.mL^{-1} (2x) and 3.2 µg.mL^{-1} (4x) of a fluorescence derivative of the cell wall dye vancomycin-FL (Van-FL) were used as a positive control. Floating bars represent minimum and maximum value of fluorescence and lines at the middle correspond to the medians.

3.6. Daptomycin fluorescence

While performing induction assays of daptomycin-challenged cultures with the *lrg* reporter strains, fluorescence of daptomycin in the DAPI channel was detected during the controls of previous assays of *lrg* reporter strains (Figure 3.16).

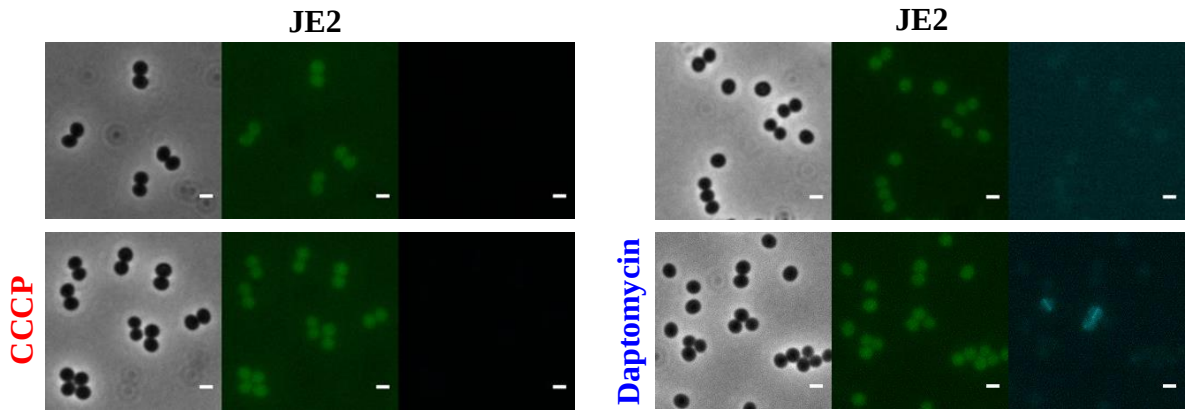

Figure 3.16. Microscopy images of JE2 exposed to CCCP and daptomycin. WT cells were incubated without and with inducer. Each three-panels from the second row show JE2 cells in the presence of CCCP and daptomycin. For each three-panel example: left – phase contrast image; middle – GFP filter image; right – DAPI filter image. Scale bars = 1 µm.

In Figure 3.16, an unexpected midcell/septal-like fluorescence pattern can be observed on the image obtained with the DAPI filter in WT JE2 cells challenged with daptomycin. However, this pattern was not common to all the cells (Figure 3.16.).

To briefly study this intriguing phenomenon, the CA-MRSA JE2 WT strain was grown in MHB and Ca-MHB and the microscopy assay was repeated. The WT strain displayed similar growth rates when comparing liquid cultures in both media with and without calcium (Supplementary Figure 4). The fluorescence of this *S. aureus* strain in the presence of daptomycin (Figure 3.17.) was assessed.

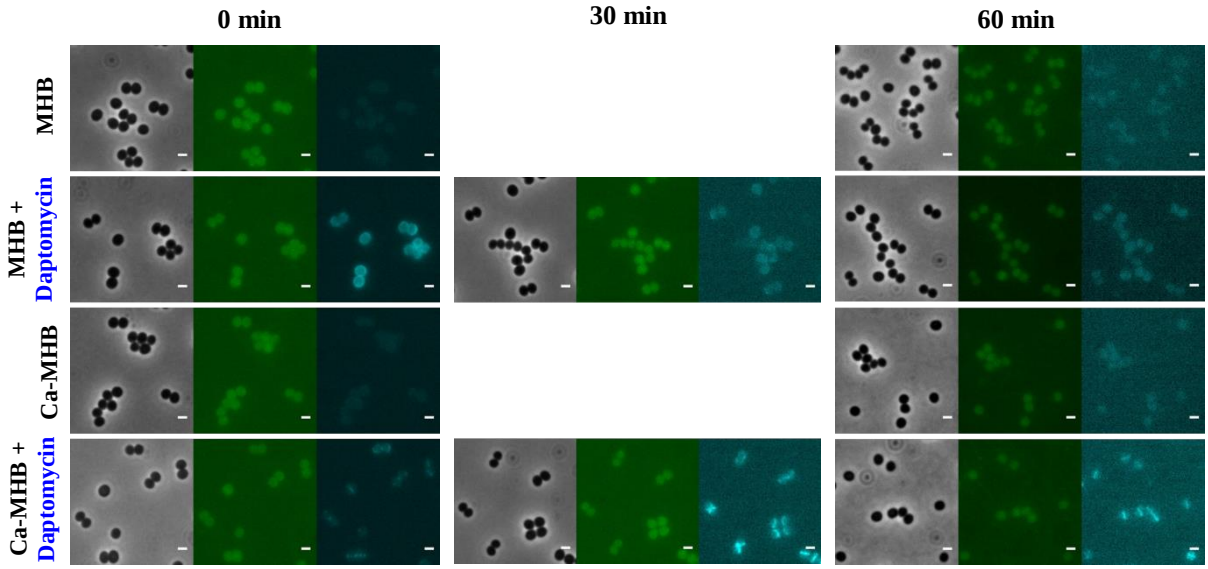

Figure 3.17. Microscopy images of JE2 exposed to daptomycin. WT cells in MHB without and with antibiotic, in Ca-MHB without and with antibiotic. Each three-panels show cells at time zero, 30 min and 1 h of growth after reaching $OD_{600\ nm} \approx 0.8$. For each three-panel example: left – phase contrast image; middle – GFP filter image; right – DAPI filter image. The GFP channel only displayed cell autofluorescence. Scale bars = 1 μm.

Data from Figure 3.17. illustrates either a whole cell surface-like labelling or a midcell/septal pattern only detectable with the DAPI filter. Interestingly, midcell labelling was exclusive to cells grown in MHB supplemented with calcium (Ca-MHB), whereas whole cell surface-like labelling pattern is more predominant in cultures grown in calcium-free MHB but still detectable in Ca-MHB. 1 h after reaching exponential phase, intensity for this staining decreased.

Importantly, daptomycin fluorescence was not detected in the GFP filter and, therefore, did not interfere with the assays described above.

To better understand how the presence of daptomycin causes these labelling patterns, further experiments are required.

4. Discussion and Conclusions

Cell membranes are vital for bacterial survival[89,117], thus have been proposed as a target for compounds which are used as treatment to multidrug resistant and persistent bacteria[20,48,77,118]. Therefore, its integrity/stability (proton motive force) and composition, namely in phospholipids, can serve as starting points to discover new compounds that affect or inhibit clinically relevant bacteria, such as *Staphylococcus aureus* USA300 (JE2). In this work, we constructed fluorescent reporter fusions to assess whether membrane potential and phospholipids biosynthesis could be insightful targets in a HTS for compounds with antibacterial activity. Every experiment was performed in constructs with the background of CA-MRSA JE2 strain to ensure that all results were relevant in this pathogen of interest.

Since proton motive force plays a key role in several metabolic pathways involving ATP synthesis[61,119], bacteria keep it monitored by a two-component regulatory system, *lytSR*[63,72]. In *S. aureus*, this system regulates the downstream dicistronic operon *lrgAB*, which is known to be activated by CCCP[72] and daptomycin[73,80]. Thus, we firstly constructed a reporter fusion of *mneongreen* to the promoter of *lrg*, by duplicating the native promoter in the JE2 background. Introduction of this construct in the genome did not alter strain growth, when compared with a WT background (Figure 3.2.A) neither its susceptibility to daptomycin or CCCP (Table 3.1). In liquid medium with agitation, the presence of CCCP abolishes the membrane potential and the number of cells in the culture decreases, even in sub-MIC conditions (Figure 3.2.A). The disruptive effect of daptomycin is not as evident as that of CCCP in line with the fact that their MOA, yet to be fully understood, seem to be different[72,73,78].

Following the expression of *lrg* genes through mNeonGreen fluorescence allowed to verify that P_{lrg} displayed increased activity only in the presence of 4x MIC of CCCP and daptomycin, from the various conditions tested. However, its activation is low comparing with previously reported transcription levels, where a 2.7 and 3.6-fold increase was measured for upregulation of *lrgA* and *lrgB* by daptomycin, respectively[73]. Daptomycin induction was heterogeneous and prolonged exposure to the inducer resulted in phenotypical alterations such as cell enlargement (Figures 3.4., 3.5. and 3.6.).

Seeing the rapid effect of CCCP in abolishing membrane potential[61,72], cultures of the reporter strain were incubated with 1x and 4x MIC of the uncoupler agent for 5 min, 10 min and 15 min after reaching early exponential phase and for 45 min with 2x MIC. However, 15 min or less for induction did not allow a comparable activation of the P_{lrg} promoter (Supplementary Figure 2). The same results were obtained for the 45 min experiment (Supplementary Figure 3).

To assess P_{lrg} promoter activation through the secondary LytS-independent pathway (Figure 1.1.) while avoiding cell enlargement, glucose and potassium acetate were used as inducers. Bicarbonate was also tested as another possible inducer of the primary/LytS-dependent pathway (Figure 1.1.) by interference with membrane potential[116]. The results in Figure 3.7. suggest that glucose acts as a repressor, which may be possible due to catabolic repression by the carbon catabolite protein A (CcpA)[120]. Potassium acetate also might have repressed the activation of P_{lrg} after 2 h of induction. Although acetate and bicarbonate did not activate the promoter, the concentrations might not have been ideal for this reporter and further testing is required.

Considering the results obtained, the reported strain containing a duplication of the P_{lrg} native promoter shows low activation levels. Therefore, an alternative strategy was considered for the *lrg* reporter (Figure 4.1.), which consisted in constructing a reporter strain by placing the *mneongreen* sequence after the *lrgB* native gene, *i.e.*, cloning the gene encoding the mNeonGreen fluorescent protein at the end of the operon *lrgAB*, to minimize disturbance of its expression. Instead of duplicating the promoter and possibly diluting the activator LytR due to having two promoter regions for the regulator to bind to, this new strategy could potentially cause an alteration in the expression of the *lrg* genes or a destabilization of the resulting transcript. Still, no perceptible changes were detected regarding MICs (Table 3.1.) or growth profiles in liquid media (Figure 3.2.B). Although the daptomycin and CCCP

induction results obtained with this strategy show an improvement to the previous construction, quantifications (Figure 3.10.) demonstrated that the fluorescence increase after induction is inferior to a two-fold difference to the positive control with non-induced culture of this alternative reporter strain. In view of the results for both strategies, we concluded that the constructed *lrg* fluorescent reporter is not adequate to be used in a HTS.

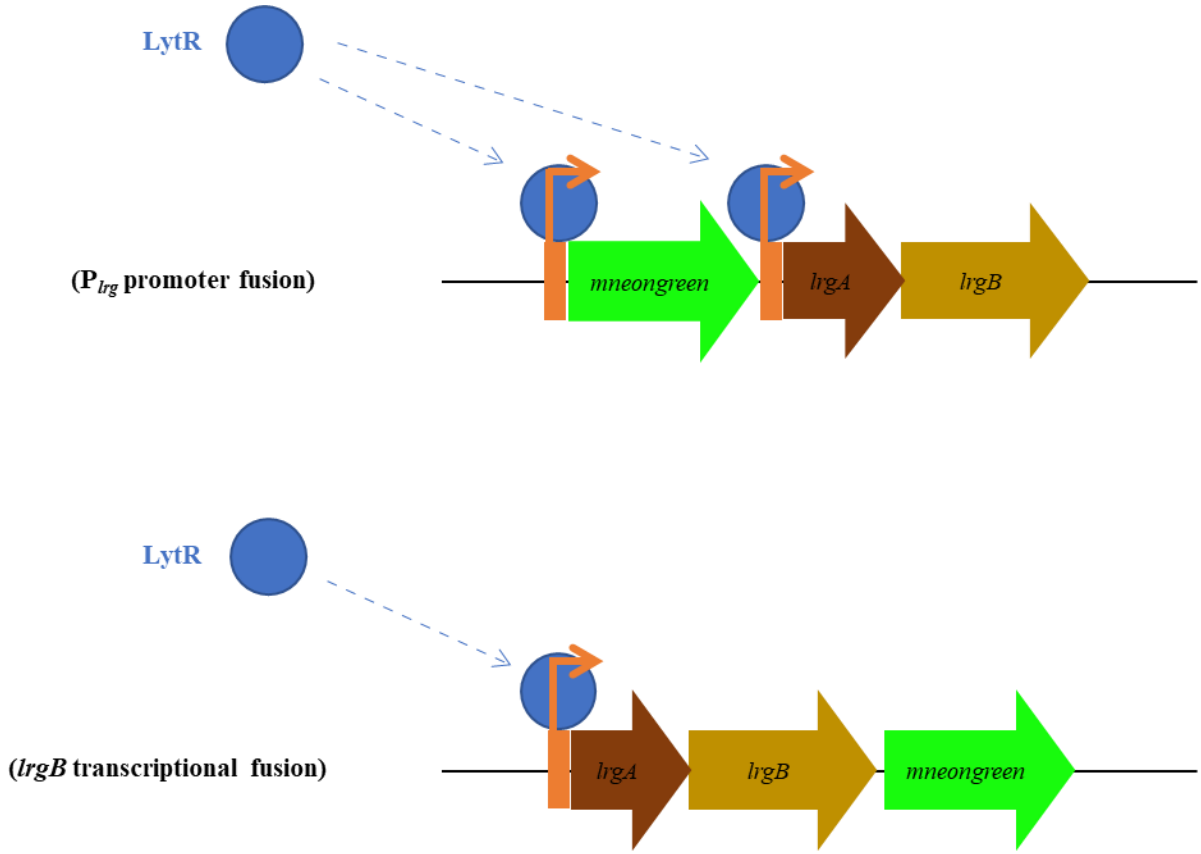

Figure 4.1. Scheme of LytR binding sites for each *lrg* reporter strategy. Duplication of the native promoters can lead to dilution of the activator LytR, decreasing expression of *mneongreen* due to existence of two LytR DNA-binding sites in the genome. On the other hand, addition of the codifying sequence for mNeonGreen fluorescent protein at the end of the operon avoids this dilution effect, allowing maintenance of a single target for the regulator protein. However, this alternative strategy can compromise mRNA stability and subsequent protein production.

Another important aspect of membranes is its phospholipids composition. The Gram-positive bacteria *S. aureus* has a FASII system to synthetize its own phospholipids[121] though it can also make use of exogenous fatty acids during host infection[97]. In order to evaluate whether the FASII could serve as a target for a fluorescent-based HTS, a fluorescent reporter fusion was also constructed by duplication of the P_{fap} promoter adjacently to the *fapR locus* (Figure 3.1.C). Contrary to the previous reporter where LytR was an activator, FapR is a transcriptional repressor whose DNA/operator-binding function is inhibited by the intermediate metabolite of FASII, malonyl-CoA[93].

To activate the *fap* reporter strain and observe if there was an increase of mNeonGreen fluorescence, triclosan was used as an inducer. The compound blocks the FabI-mediated step of the elongation cycle of bacterial FASII (Figure 1.3.), leading to malonyl-CoA accumulation and consequently loss of FapR repression[121]. Similarly to the first set of experiments with the *lrg* reporter, duplication of the native promoter did not change growth (Figure 3.3.) nor resistance (Table 3.1.). In

liquid media, triclosan induction resulted in almost a two-fold increase of mNeonGreen fluorescence levels during the first hour (Figure 3.13.).

The second approach used to validate the reporter strain was based on a xylose-inducible RNA antisense system against *fabZ*. In the absence of FabZ, the conversion of β-hydroxyacyl-ACP to trans-2-enoyl-ACP (Figure 1.3.) is blocked, which leads to the accumulation of intracellular malonyl-CoA and a decrease of FapR-mediated repression. Hence with this approach, fluorescence quantification of xylose-induced cells demonstrated that the P_{fap} promoter could be activated by targeting a different gene of the fatty acid synthesis pathway/cycle, being therefore a useful reporter for new antimicrobials.

Taking together these results, the *fap* reporter strain was considered promising for a HTS based on a fluorimeter microplate system. However, differences in fluorescence levels detected during the testing of the reporter in the fluorimeter did not correlate with data from microscopy analysis. A possible explanation may be the 200-fold scale-up from the sample volume used in microscopy to the volume usually used in microplate assays.

Triclosan-induced cells exhibited fluorescence levels below the minimum detection limit of the fluorimeter. This was evaluated by the vancomycin-labelling of WT parental strain. Additionally, the $OD_{600\ nm}$ adjustments to 0.1 mentioned in Results reduced the total amount of cells in each microplate well, which consequently decreased total mNeonGreen protein available in the sample.

Interestingly, while doing the studies described in this thesis, a daptomycin fluorescence signal was detected on the DAPI filter. It has been reported that the kynurenine aminoacid of this lipopeptide undergoes a blue shift upon interaction with calcium and negatively charged phospholipid membranes, namely with PG in its composition. A weaker shift in the fluorescence can also happen with neutral membranes[86]. Although this explains the signal detected in Figures 3.16. and 3.17., it does not justify the different staining patterns: the midcell pattern indicated that Ca-Dap complexes may bind to the septum of *S. aureus* cells, while in the absence of this cation daptomycin can also label the whole cell surface of the bacteria. Still, further research on this subject is required. Due to this fluorescence (Figure 3.16), the assays with daptomycin induction were repeated by staining the induced-cells instead of the positive control (non-induced *lrg* reporter cells). Quantification of these results (data not shown) allowed to conclude that daptomycin blue-shit did not interfere with analysis of mNeonGreen fluorescence levels from previously discussed results of *lrg* reporter strains constructed in this work.

In conclusion, a fluorescence based HTS using the *fap* reporter could be useful to identify new compounds and study their mode of action on MRSA *S. aureus* strains. Yet, an alternative to overcome detection limits of the mNeonGreen fluorescence would be to construct these reporters with bacterial luciferase (*lux* genes) and monitor promoter activities by measuring luminescence levels, as using this technique in target-based reporter assays may provide better results with higher sensitivity[122].

5. References

1. Stryjewski, M. E. & Corey, G. R. Methicillin-resistant *Staphylococcus aureus*: An evolving pathogen. *Clin. Infect. Dis.* **58,** 10–19 (2014).
2. Boucher, H., Miller, L. G. & Razonable, R. R. Serious Infections Caused by Methicillin-Resistant *Staphylococcus aureus*. *Clin. Infect. Dis.* **51,** S183–S197 (2010).
3. Wertheim, H. F. *et al.* The role of nasal carriage in *Staphylococcus aureus* infections. *Lancet Infect. Dis.* **5,** 751–762 (2005).
4. Gordon, R. J. & Lowy, F. D. Pathogenesis of Methicillin-Resistant *Staphylococcus aureus* Infection. *Clin. Infect. Dis.* **46,** S350–S359 (2008).
5. Thompson, R., Cabezudo, I., Wenzel, R. & Thompson I.: Wenzel, R. P., R. L. . C. Epidemiology of nosocomial infections caused by methicillin-resistant *Staphylococcus aureus*. *Ann med interna* **97,** 309–17 (1982).
6. Kazakova, S. V *et al.* A Clone of Methicillin-Resistant *Staphylococcus aureus* among Professional Football Players. *N. Engl. J. Med.* **352,** 468–475 (2005).
7. Miller, L. G. & Diep, B. A. Colonization, Fomites, and Virulence: Rethinking the Pathogenesis of Community-Associated Methicillin-Resistant *Staphylococcus aureus* Infection. *Clin. Infect. Dis.* **46,** 752–760 (2008).
8. van Hal, S. J. *et al.* Predictors of mortality in *Staphylococcus aureus* bacteremia. *Clin. Microbiol. Rev.* **25,** 362–386 (2012).
9. van Heijenoort, J. Assembly of the monomer unit of bacterial peptidoglycan. *Cell. Mol. Life Sci. C.* **54,** 300–304 (1998).
10. Scheffers, D.-J. & Pinho, M. G. Bacterial Cell Wall Synthesis: New Insights from Localization Studies. *Microbiol. Mol. Biol. Rev.* **69,** 585–607 (2005).
11. Ligon, B. L. Penicillin: Its Discovery and Early Development. *Semin. Pediatr. Infect. Dis.* **15,** 52–57 (2004).
12. Barber, M. & Rozwadowska-Dowzenko, M. Infection by penicillin-resistant staphylococci. *Lancet* **252,** 641–644 (1987).
13. Bondi, A. J. & Dietz, C. C. Penicillin Resistant Staphylococci. *Proc. Soc. Exp. Biol. Med.* **60,** 55–58 (1945).
14. Lowy, F. D. Antimicrobial resistance: the example of *Staphylococcus aureus*. *J. Clin. Invest.* **111,** 1265–1273 (2003).
15. Shanson, D. C. Antibiotic-resistant *Staphylococcus aureus*. *J. Hosp. Infect.* **2,** 11–36 (1981).
16. Jevons, M. P. "Celbenin" - resistant Staphylococci. *Br. Med. J.* **1,** 124–125 (1961).
17. Jevons, M. P., Coe, A. W. & Parker, M. T. Methicillin Resistance in Staphylococci. *Lancet* **281,** 904–907 (1963).
18. Seligman, S. J. Penicillinase-Negative Variants of Methicillin-Resistant *Staphylococcus aureus*. *Nature* **209,** 994–996 (1966).
19. Lyon, B. R. & Skurray, R. Antimicrobial resistance of *Staphylococcus aureus*: genetic basis. *Microbiol. Rev.* **51,** 88–134 (1987).
20. Foster, T. J. Antibiotic resistance in *Staphylococcus aureus*. Current status and future prospects. *FEMS Microbiol. Rev.* **41,** 430–449 (2017).
21. Saravolatz, L. D., Markowitz, N., Arking, L., Pohlod, D., Fisher, E. Methicillin-resistant *Staphylococcus aureus*: Epidemiologic observations during a community-acquired outbreak. *Ann. Intern. Med.* **96,** 11–16 (1982).
22. Moran, G. J. *et al.* Methicillin-Resistant *S. aureus* Infections among Patients in the Emergency Department. *N. Engl. J. Med.* **355,** 666–674 (2006).
23. Rudkin, J. K. *et al.* Methicillin Resistance Reduces the Virulence of Healthcare-Associated Methicillin-Resistant *Staphylococcus aureus* by Interfering With the agr Quorum Sensing System. *J. Infect. Dis.* **205,** 798–806 (2012).
24. Chambers, H. F. & DeLeo, F. R. Waves of Resistance: *Staphylococcus aureus* in the Antibiotic Era. *Nat. Rev. Microbiol.* **7,** 629–641 (2009).
25. Kennedy, A. D. *et al.* Epidemic community-associated methicillin-resistant *Staphylococcus aureus*: Recent clonal expansion and diversification. *Proc. Natl. Acad. Sci. U. S. A.* **105,** 1327–1332 (2008).

26. Seybold, U. *et al.* Emergence of Community-Associated Methicillin-Resistant *Staphylococcus aureus* USA300 Genotype as a Major Cause of Health Care—Associated Blood Stream Infections. *Clin. Infect. Dis.* **42,** 647–656 (2006).
27. Tenover, F. C. & Goering, R. V. Methicillin-resistant *Staphylococcus aureus* strain USA300: origin and epidemiology. *J. Antimicrob. Chemother.* **64,** 441–446 (2009).
28. Klevens, R., MA, M., Nadle, J. & al, et. Invasive methicillin-resistant *Staphylococcus aureus* infections in the united states. *JAMA* **298,** 1763–1771 (2007).
29. Shibuya, Y. *et al.* Emergence of the community-acquired methicillin-resistant *Staphylococcus aureus* USA300 clone in Japan. *J. Infect. Chemother.* **14,** 439–441 (2008).
30. Park, C. *et al.* A Case of Perianal Abscess due to Panton-Valentine Leukocidin Positive Community-Associated Methicillin-Resistant *Staphylococcus aureus*: Report in Korea and Literature Review from the Far East. *Infect Chemother* **40,** 121–126 (2008).
31. Gottlieb, T., Su, W. Y., Merlino, J. & Cheong, E. Y. L. Recognition of USA300 isolates of community-acquired methicillin-resistant *Staphylococcus aureus* in Australia. *Med. J. Aust.* **189,** 179–180 (2008).
32. Zeng, D. *et al.* Approved glycopeptide antibacterial drugs: Mechanism of action and resistance. *Cold Spring Harb. Perspect. Med.* **6,** (2016).
33. Hiramatsu, K. *et al.* Dissemination in Japanese hospitals of strains of *Staphylococcus aureus* heterogeneously resistant to vancomycin. *Lancet* **350,** 1670–1673 (1997).
34. Weigel, L. M. *et al.* Genetic Analysis of a High-Level Vancomycin-Resistant Isolate of *Staphylococcus aureus*. *Science (80-.).* **302,** 1569 LP-1571 (2003).
35. Hageman, J. C. *et al.* Occurrence of a USA300 vancomycin-intermediate *Staphylococcus aureus*. *Diagn. Microbiol. Infect. Dis.* **62,** 440–442 (2008).
36. Stefani, S. *et al.* Insights and clinical perspectives of daptomycin resistance in *Staphylococcus aureus*: A review of the available evidence. *Int. J. Antimicrob. Agents* **46,** 278–289 (2015).
37. Bayer, A. S., Schneider, T. & Sahl, H.-G. Mechanisms of daptomycin resistance in *Staphylococcus aureus*: role of the cell membrane and cell wall. *Ann. N. Y. Acad. Sci.* **1277,** 139–158 (2013).
38. Pader, V. *et al. Staphylococcus aureus* inactivates daptomycin by releasing membrane phospholipids. *Nat. Microbiol.* **2,** (2016).
39. Long, K. S. & Vester, B. Resistance to Linezolid Caused by Modifications at Its Binding Site on the Ribosome. *Antimicrob. Agents Chemother.* **56,** 603 LP-612 (2012).
40. Davies, J. & Davies, D. Origins and Evolution of Antibiotic Resistance. *Microbiol. Mol. Biol. Rev.* **74,** 417–433 (2010).
41. Laxminarayan, R. *et al.* Antibiotic resistance - the need for global solutions. *Lancet Infect. Dis.* **13,** 1057–1098 (2013).
42. Boucher, H. W. & Corey, G. R. Epidemiology of Methicillin-Resistant *Staphylococcus aureus*. *Clin. Infect. Dis.* **46,** S344–S349 (2008).
43. Rolo, J. *et al.* High Genetic Diversity among Community-Associated *Staphylococcus aureus* in Europe: Results from a Multicenter Study. *PLoS One* **7,** e34768 (2012).
44. Fernandes, P. A., Silva, M. G., Cruz, A. P. & Paiva, J. A. *Portugal - Prevenção e Controlo de Infeções e de Resistência aos Antimicrobianos em números - 2015*. *Direção Geral da Saúde* (2016).
45. Fischbach, M. A. & Walsh, C. T. Antibiotics For Emerging Pathogens. *Science (80-.).* **325,** 1089–1093 (2009).
46. Silver, L. L. Challenges of Antibacterial Discovery. *Clin. Microbiol. Rev.* **24,** 71–109 (2011).
47. Farha, M. A. & Brown, E. D. Strategies for target identification of antimicrobial natural products. *Nat. Prod. Rep.* **33,** 668–680 (2016).
48. Farha, M. A. & Brown, E. D. Unconventional screening approaches for antibiotic discovery. *Ann. N. Y. Acad. Sci.* **1354,** 54–66 (2015).
49. Payne, D. J., Gwynn, M. N., Holmes, D. J. & Pompliano, D. L. Drugs for bad bugs: confronting the challenges of antibacterial discovery. *Nat. Rev. Drug Discov.* **6,** 29 (2006).
50. Van Der Meer, J. R. & Belkin, S. Where microbiology meets microengineering: Design and applications of reporter bacteria. *Nat. Rev. Microbiol.* **8,** 511–522 (2010).
51. Melamed, S. *et al.* A bacterial reporter panel for the detection and classification of antibiotic

substances. *Microb. Biotechnol.* **5,** 536–548 (2012).
52. Valtonen, S. J., Kurittu, J. S. & Karp, M. T. A Luminescent *Escherichia coli* Biosensor for the High Throughput Detection of β-Lactams. *J. Biomol. Screen.* **7,** 127–134 (2002).
53. Malone, C. L. *et al.* Fluorescent Reporters for *Staphylococcus aureus*. *J. Microbiol. Methods* **77,** 251–260 (2009).
54. Pereira, P. M., Veiga, H., Jorge, A. M. & Pinho, M. G. Fluorescent reporters for studies of cellular localization of proteins in *Staphylococcus aureus*. *Appl. Environ. Microbiol.* **76,** 4346–4353 (2010).
55. de Jong, N. W. M., van der Horst, T., van Strijp, J. A. G. & Nijland, R. Fluorescent reporters for markerless genomic integration in *Staphylococcus aureus* . *Sci. Rep.* **7,** 43889 (2017).
56. Urban, A. *et al.* Novel Whole-Cell Antibiotic Biosensors for Compound Discovery . *Appl. Environ. Microbiol.* **73,** 6436–6443 (2007).
57. Ling, L. L. *et al.* A new antibiotic kills pathogens without detectable resistance. *Nature* **517,** 455–459 (2015).
58. Homma, T. *et al.* Dual Targeting of Cell Wall Precursors by Teixobactin Leads to Cell Lysis. *Antimicrob. Agents Chemother.* **60,** 6510 LP-6517 (2016).
59. Wu, X. & Hurdle, J. G. Screening for a Diamond in the Rough. *Chem. Biol.* **20,** 1091–1092 (2013).
60. Farha, M. A., Verschoor, C. P., Bowdish, D. & Brown, E. D. Collapsing the proton motive force to identify synergistic combinations against *Staphylococcus aureus*. *Chem. Biol.* **20,** 1168–1178 (2013).
61. Strahl, H. & Hamoen, L. W. Membrane potential is important for bacterial cell division. *Proc. Natl. Acad. Sci.* **107,** 12281–12286 (2010).
62. Brunskill, E. W. & Bayles, K. W. Identification and molecular characterization of a putative regulatory *locus* that affects autolysis in *Staphylococcus aureus*. *J. Bacteriol.* **178,** 611–618 (1996).
63. Yang, S. J. *et al.* Role of the LytSR two-component regulatory system in adaptation to cationic antimicrobial peptides in *Staphylococcus aureus*. *Antimicrob. Agents Chemother.* **57,** 3875–3882 (2013).
64. Patel, K. & Golemi-Kotra, D. Signaling mechanism by the *Staphylococcus aureus* two-component system LytSR: role of acetyl phosphate in bypassing the cell membrane electrical potential sensor LytS. *F1000Research* **4,** 79 (2015).
65. Lehman, M. K. *et al.* Identification of the amino acids essential for LytSR-mediated signal transduction in *Staphylococcus aureus* and their roles in biofilm-specific gene expression. *Mol. Microbiol.* **95,** 723–737 (2015).
66. Brunskill, E. W. & Bayles, K. W. Identification of LytSR-regulated genes from *Staphylococcus aureus*. *J. Bacteriol.* **178,** 5810–5812 (1996).
67. Groicher, K. H., Firek, B. A., Fujimoto, D. F. & Bayles, K. W. The *Staphylococcus aureus lrgAB* operon modulates murein hydrolase activity and penicillin tolerance. *J. Bacteriol.* **182,** 1794–1801 (2000).
68. Bayles, K. W. The biological role of death and lysis in biofilm development. *Nat. Rev. Microbiol.* **5,** 721–726 (2007).
69. Rice, K. C. & Bayles, K. W. Molecular Control of Bacterial Death and Lysis. *Microbiol. Mol. Biol. Rev.* **72,** 85–109 (2008).
70. Rice, K. C. & Bayles, K. W. Death's toolbox: examining the molecular components of bacterial programmed cell death. *Mol. Microbiol.* **50,** 729–738 (2003).
71. van den Esker, M. H., Kovács, Á. T. & Kuipers, O. P. From Cell Death to Metabolism: Holin-Antiholin Homologues with New Functions. *MBio* **8,** e01963-17 (2017).
72. Patton, T. G., Yang, S.-J. & Bayles, K. W. The role of proton motive force in expression of the *Staphylococcus aureus cid* and *lrg* operons. *Mol. Microbiol.* **59,** 1395–1404 (2006).
73. Muthaiyan, A., Silverman, J. A., Jayaswal, R. K. & Wilkinson, B. J. Transcriptional profiling reveals that daptomycin induces the *Staphylococcus aureus* cell wall stress stimulon and genes responsive to membrane depolarization. *Antimicrob. Agents Chemother.* **52,** 980–990 (2008).
74. Sharma-Kuinkel, B. K. *et al.* The *Staphylococcus aureus* LytSR two-component regulatory system affects biofilm formation. *J. Bacteriol.* **191,** 4767–4775 (2009).

75. Arbeit, R. D. *et al.* The Safety and Efficacy of Daptomycin for the Treatment of Complicated Skin and Skin-Structure Infections. *Clin. Infect. Dis.* **38,** 1673–1681 (2004).
76. Hawkey, P. M. Pre-clinical experience with daptomycin. *J. Antimicrob. Chemother.* **62,** iii7-iii14 (2008).
77. Bush, K. Antimicrobial agents targeting bacterial cell walls and cell membranes. *Rev. Sci. Tech.* **31,** 43–56 (2012).
78. Silverman, J. a, Perlmutter, N. G., Howard, M. & Shapiro, H. M. Correlation of daptomycin bactericidal activity and membrane depolarization in *Staphylococcus aureus*. *Antimicrob. Agents Chemother.* **47,** 2538–2544 (2003).
79. Hachmann, A.-B. *et al.* Reduction in Membrane Phosphatidylglycerol Content Leads to Daptomycin Resistance in *Bacillus subtilis* . *Antimicrob. Agents Chemother.* **55,** 4326–4337 (2011).
80. Friedman, L., Alder, J. D. & Silverman, J. A. Genetic Changes That Correlate with Reduced Susceptibility to Daptomycin in *Staphylococcus aureus* . *Antimicrob. Agents Chemother.* **50,** 2137–2145 (2006).
81. Palmer, K. L., Daniel, A., Hardy, C., Silverman, J. & Gilmore, M. S. Genetic Basis for Daptomycin Resistance in Enterococci. *Antimicrob. Agents Chemother.* **55,** 3345–3356 (2011).
82. Rubio, A. *et al.* Regulation of *mprF* by Antisense RNA Restores Daptomycin Susceptibility to Daptomycin-Resistant Isolates of *Staphylococcus aureus*. *Antimicrob. Agents Chemother.* **55,** 364 LP-367 (2011).
83. Davlieva, M., Zhang, W., Arias, C. A. & Shamoo, Y. Biochemical Characterization of Cardiolipin Synthase Mutations Associated with Daptomycin Resistance in Enterococci. *Antimicrob. Agents Chemother.* **57,** 289–296 (2013).
84. Mishra, N. N. *et al.* Carotenoid-Related Alteration of Cell Membrane Fluidity Impacts *Staphylococcus aureus* Susceptibility to Host Defense Peptides. *Antimicrob. Agents Chemother.* **55,** 526–531 (2011).
85. Cotroneo, N., Harris, R., Perlmutter, N., Beveridge, T. & Silverman, J. A. Daptomycin exerts bactericidal activity without lysis of *Staphylococcus aureus*. *Antimicrob. Agents Chemother.* **52,** 2223–2225 (2008).
86. Muraih, J. K., Pearson, A., Silverman, J. & Palmer, M. Oligomerization of daptomycin on membranes. *Biochim. Biophys. Acta - Biomembr.* **1808,** 1154–1160 (2011).
87. Mishra, N. N. *et al.* Phenotypic and Genotypic Characterization of Daptomycin-Resistant Methicillin-Resistant *Staphylococcus aureus* Strains: Relative Roles of mprF and dlt Operons. *PLoS One* **9,** e107426 (2014).
88. Hachmann, A.-B., Angert, E. R. & Helmann, J. D. Genetic Analysis of Factors Affecting Susceptibility of *Bacillus subtilis* to Daptomycin. *Antimicrob. Agents Chemother.* **53,** 1598–1609 (2009).
89. Parsons, J. B. & Rock, C. O. Is bacterial fatty acid synthesis a valid target for antibacterial drug discovery? *Curr. Opin. Microbiol.* **14,** 544–549 (2011).
90. Yao, J. & Rock, C. O. How Bacterial Pathogens Eat Host Lipids: Implications for the Development of Fatty Acid Synthesis Therapeutics. *J. Biol. Chem.* **290,** 5940–5946 (2015).
91. Schujman, G. E., Paoletti, L., Grossman, A. D. & de Mendoza, D. FapR, a bacterial transcription factor involved in global regulation of membrane lipid biosynthesis. *Dev. Cell* **4,** 663–672 (2003).
92. Schujman, G. E. *et al.* Structural basis of lipid biosynthesis regulation in Gram-positive bacteria. *EMBO J.* **25,** 4074–4083 (2006).
93. Albanesi, D. *et al.* Structural Basis for Feed-Forward Transcriptional Regulation of Membrane Lipid Homeostasis in *Staphylococcus aureus*. *PLoS Pathog.* **9.** (2013).
94. Heath, R. J., Yu, Y., Shapiro, M. A., Olson, E. & Rock, C. O. Broad Spectrum Antimicrobial Biocides Target the FabI Component of Fatty Acid Synthesis. *J. Biol. Chem.* **273,** 30316–30320 (1998).
95. Schiebel, J. *et al. Staphylococcus aureus* FabI: Inhibition, Substrate Recognition, and Potential Implications for *In Vivo* Essentiality. *Structure* **20,** 802–813 (2012).
96. Ciusa, M. L. *et al.* A novel resistance mechanism to triclosan that suggests horizontal gene transfer and demonstrates a potential selective pressure for reduced biocide susceptibility in

clinical strains of *Staphylococcus aureus*. *Int. J. Antimicrob. Agents* **40,** 210–220 (2012).
97. Delekta, P. C., Shook, J. C., Lydic, T. A., Mulks, M. H. & Hammer, N. D. *Staphylococcus aureus* utilizes host-derived lipoprotein particles as sources of exogenous fatty acids. *J. Bacteriol.* JB.00728-17 (2018).
98. Brinster, S. *et al.* Type II fatty acid synthesis is not a suitable antibiotic target for Gram-positive pathogens. *Nature* **458,** 83–86 (2009).
99. Balemans, W. *et al.* Essentiality of FASII pathway for *Staphylococcus aureus*. *Nature* **463,** E1–E1 (2010).
100. Park, H. S. *et al.* Antistaphylococcal activities of CG400549, a new bacterial enoyl-acyl carrier protein reductase (FabI) inhibitor. *J. Antimicrob. Chemother.* **60,** 568–574 (2007).
101. Escaich, S. *et al.* The MUT056399 Inhibitor of FabI Is a New Antistaphylococcal Compound. *Antimicrob. Agents Chemother.* **55,** 4692 LP-4697 (2011).
102. Yao, J. & Rock, C. O. Resistance Mechanisms and the Future of Bacterial Enoyl-Acyl Carrier Protein Reductase (FabI) Antibiotics. *Cold Spring Harb. Perspect. Med.* **6,** a027045–a027045 (2016).
103. Monk, I. R., Shah, I. M., Xu, M., Tan, M.-W. & Foster, T. J. Transforming the Untransformable: Application of Direct Transformation To Manipulate Genetically *Staphylococcus aureus* and *Staphylococcus epidermidis*. *MBio* **3,** e00277-11 (2012).
104. Nair, D. *et al.* Whole-genome sequencing of *Staphylococcus aureus* strain RN4220, a key laboratory strain used in virulence research, identifies mutations that affect not only virulence factors but also the fitness of the strain. *J. Bacteriol.* **193,** 2332–2335 (2011).
105. Diep, B. A. *et al.* Complete genome sequence of USA300, an epidemic clone of community-acquired meticillin-resistant *Staphylococcus aureus*. *Lancet* **367,** 731–739 (2006).
106. Arnaud, M., Chastanet, A. & De, M. New Vector for Efficient Allelic Replacement in Naturally Gram-Positive Bacteria New Vector for Efficient Allelic Replacement in Naturally Gram-Positive Bacteria. *Appl. Enviromental Microbiol.* **70,** 6887–6891 (2004).
107. Donald, R. G. K. K. *et al.* A *Staphylococcus aureus* Fitness Test Platform for Mechanism-Based Profiling of Antibacterial Compounds. *Chem. Biol.* **16,** 826–836 (2009).
108. Gibson, D. G. *et al.* Enzymatic assembly of DNA molecules up to several hundred kilobases. *Nat. Methods* **6,** 343–345 (2009).
109. Kraemer, G. R. & Iandolo, J. J. High-frequency transformation of *Staphylococcus aureus* by electroporation. *Curr. Microbiol.* **21,** 373–376 (1990).
110. Oshida, T. & Tomasz, A. Isolation and characterization of a Tn551-autolysis mutant of *Staphylococcus aureus*. *J. Bacteriol.* **174,** 4952–4959 (1992).
111. Monteiro, J. M. *et al.* Peptidoglycan synthesis drives an FtsZ-treadmilling-independent step of cytokinesis. *Nature* **554,** 528–532 (2018).
112. Monteiro, J. M. *et al.* Cell shape dynamics during the staphylococcal cell cycle. *Nat. Commun.* **6,** 8055 (2015).
113. Lee, Y. J., Hoynes-O'Connor, A., Leong, M. C. & Moon, T. S. Programmable control of bacterial gene expression with the combined CRISPR and antisense RNA system. *Nucleic Acids Res.* **44,** 2462–2473 (2016).
114. Shaner, N. C. *et al.* A bright monomeric green fluorescent protein derived from *Branchiostoma lanceolatum* . *Nat. Methods* **10,** 407–409 (2013).
115. Rice, K. C., Nelson, J. B., Patton, T. G., Yang, S.-J. & Bayles, K. W. Acetic acid induces expression of the *Staphylococcus aureus cidABC* and *lrgAB* murein hydrolase regulator operons. *J. Bacteriol.* **187,** 813–821 (2005).
116. Farha, M. A., French, S., Stokes, J. M. & Brown, E. D. Bicarbonate Alters Bacterial Susceptibility to Antibiotics by Targeting the Proton Motive Force. *ACS Infect. Dis.* **4,** 382–390 (2018).
117. Herzog, I. M. *et al.* 6′′-Thioether Tobramycin Analogues: Towards Selective Targeting of Bacterial Membranes. *Angew. Chemie I(nternational Ed. English)* **51,** 5652–5656 (2012).
118. Hurdle, J. G., O'Neill, A. J., Chopra, I. & Lee, R. E. Targeting bacterial membrane function: an underexploited mechanism for treating persistent infections. *Nat. Rev. Microbiol.* **9,** 62 (2010).
119. Hurdle, J. G., O'Neill, A. J., Chopra, I. & Lee, R. E. Targeting bacterial membrane function: an underexploited mechanism for treating persistent infections. *Nat. Rev. Microbiol.* **9,** 62–75

(2011).
120. Ahn, S.-J., Rice, K. C., Oleas, J., Bayles, K. W. & Burne, R. A. The *Streptococcus mutans* Cid and Lrg systems modulate virulence traits in response to multiple environmental signals. *Microbiology* **156,** 3136–3147 (2010).
121. Parsons, J. B. *et al.* Perturbation of *Staphylococcus aureus* gene expression by the enoyl-acyl carrier protein reductase inhibitor AFN-1252. *Antimicrob. Agents Chemother.* **57,** 2182–2190 (2013).
122. Nybond, S., Karp, M. & Tammela, P. Antimicrobial assay optimization and validation for HTS in 384-well format using a bioluminescent *E. coli* K-12 strain. *Eur. J. Pharm. Sci.* **49,** 782–789 (2013).

6. Supplementary Information

Supplementary Table 1. MICs of reporter strains to compounds that affect membrane potential or fatty acid biosynthesis in TSB. For each compound, MIC was determined by microdilution method in TSB and values were obtained based on the average of three independent experiments.

Strain	CCCP MIC (µg.mL^{-1})	Daptomycin[b] MIC (µg.mL^{-1})	Triclosan MIC (µg.mL^{-1}; 24h)	Triclosan MIC (µg.mL^{-1}; 48h)
JE2	1	2	7.8×10^{-3}	6.25×10^{-2}
JE2_Plrg_mNeonGreen	1	2		
JE2_lrgB_mNeonGreen	1	1		
JE2_Pfap_mNeonGreen			7.8×10^{-3}	6.25×10^{-2}

[b]MICs determined in: TSB supplemented with 50 mg.L^{-1} of Ca^{2+}

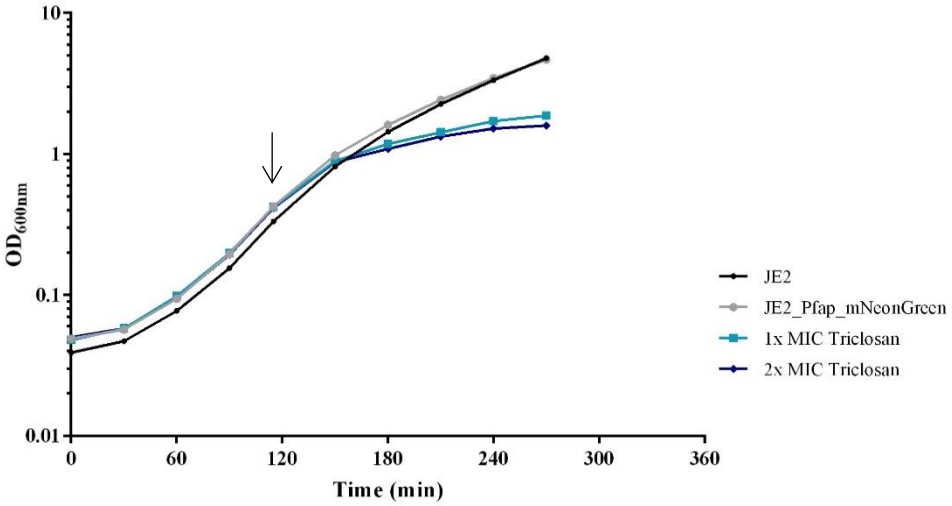

Supplementary Figure 1. Growth curves of P_{fap} reporter strain in TSB. Cultures from JE2_Pfap_mNeonGreen were grown overnight in TSB at 37 °C, re-inoculated in fresh media and regular measurements of optical density at 600nm were made. Time of induction with appropriate concentration of triclosan is indicated by the black arrow.

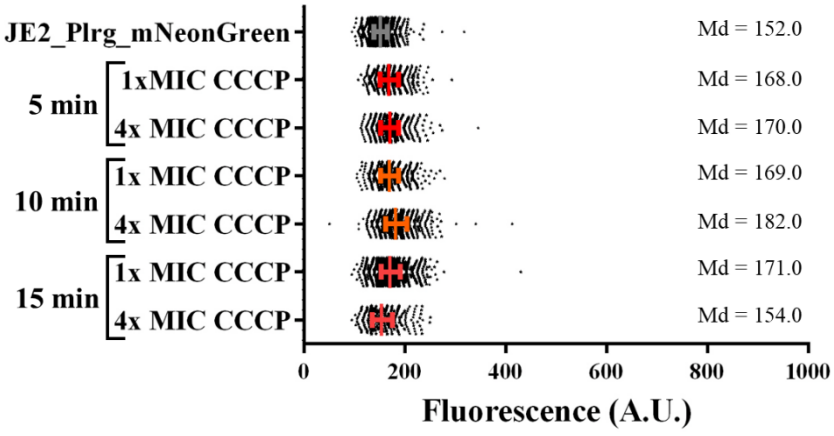

Supplementary Figure 2. P_{lrg} promoter activity in the absence or presence of CCCP during short periods of incubation. JE2_Plrg_mNeonGreen cells were challenged with 1x and 4x MIC of CCCP during 5, 10 and 15 min of induction, after cultures reached $OD_{600nm} \approx 0.4–0.5$. Each quantified cell is represented by a dot in the graphics. Grey and coloured lines represent median (Md) with interquartile range for samples with non-induced and induced cells, respectively. The median value for each tested condition is indicated.

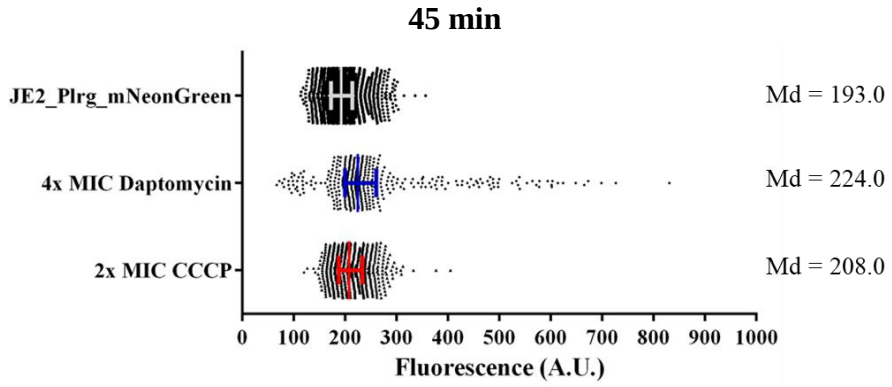

Supplementary Figure 3. P_{lrg} promoter activity in the absence or presence of supra-MIC conditions of inducer during 45 min. JE2_Plrg_mNeonGreen cells were challenged with 4x MIC of CCCP and 2x daptomycin of CCCP during 45 min of induction, after cultures reached $OD_{600nm} \approx 0.4–0.5$. Each quantified cell is represented by a dot in the graphics. Grey and coloured lines represent median (Md) with interquartile range for samples with non-induced and induced cells, respectively. The median value for each tested condition is indicated.

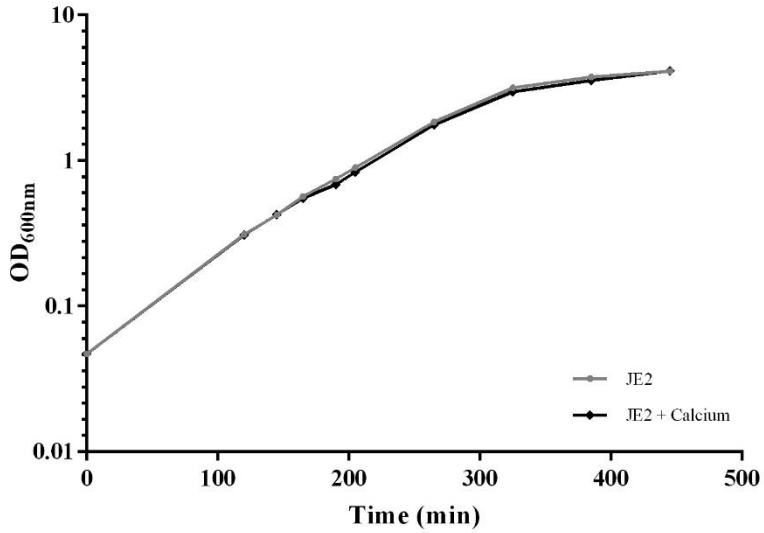

Supplementary Figure 4. Growth curves of JE2 in both MHB and Ca-MHB. Cultures of JE2 were grown overnight in MHB and MHB supplemented with 50 $mg.L^{-1}$ of Ca^{2+} at 37 °C, re-inoculated in fresh media and regular measurements of optical density at 600nm were made.